

Kiwifruit MYBS1-like and GBF3 transcription factors influence L-ascorbic acid biosynthesis by activating transcription of *GDP-L-galactose phosphorylase 3*

Xiaoying Liu^{1,2}, Rongmei Wu³, Sean M. Bulley⁴ , Caihong Zhong^{1,2} and Dawei Li^{1,2} 

¹Wuhan Botanical Garden, Chinese Academy of Sciences, Jiufeng 1 Road, Wuhan 430074, Hubei, China; ²College of Life Sciences, University of Chinese Academy of Sciences, 19A Yuquan Road, Beijing 100049, China; ³The New Zealand Institute for Plant and Food Research Limited, 120 Mt Albert Road, Mt Albert, Auckland 1025, New Zealand; ⁴The New Zealand Institute for Plant and Food Research Limited, 412 No 1 Rd, RD2, Te Puke 3182, New Zealand

Authors for correspondence:

Dawei Li

Email: lidawei@wbpcas.cn

Caihong Zhong

Email: caihongzhong@wbpcas.cn

Sean M. Bulley

Email: sean.bulley@plantandfood.co.nz

Received: 6 December 2021

Accepted: 23 February 2022

New Phytologist (2022) 234: 1782–1800

doi: 10.1111/nph.18097

Key words: abscisic acid (ABA), *Actinidia*, ascorbate, fruit, GDP-galactose phosphorylase, *Nicotiana benthamiana*, vitamin C.

Summary

- Plant-derived Vitamin C (L-ascorbic acid (AsA)) is crucial for human health and wellbeing and thus increasing AsA content is of interest to plant breeders. In plants GDP-L-galactose phosphorylase (*GGP*) is a key biosynthetic control step and here evidence is presented for two new transcriptional activators of *GGP*.
- AsA measurement, transcriptomics, transient expression, hormone application, gene editing, yeast 1/2-hybrid, and electromobility shift assay (EMSA) methods were used to identify two positively regulating transcription factors.
- *AceGGP3* was identified as the most highly expressed *GGP* in *Actinidia eriantha* fruit, which has high fruit AsA. A gene encoding a 1R-subtype myeloblastosis (MYB) protein, *AceMYBS1*, was found to bind the *AceGGP3* promoter and activate its expression. Overexpression and gene-editing show *AceMYBS1* effectively increases AsA accumulation. The bZIP transcription factor *AceGBF3* (a G-box binding factor), also was shown to increase AsA content, and was confirmed to interact with *AceMYBS1*. Co-expression experiments showed that *AceMYBS1* and *AceGBF3* additively promoted *AceGGP3* expression. Furthermore, *AceMYBS1*, but not *GBF3*, was repressed by abscisic acid, resulting in reduced *AceGGP3* expression and accumulation of AsA.
- This study sheds new light on the roles of MYBS1 homologues and ABA in modulating AsA synthesis, and adds to the understanding of mechanisms underlying AsA accumulation.

Introduction

In plants, L-ascorbic acid (AsA; vitamin C) is a major antioxidant with roles in photosynthesis, respiration, cell division, growth regulation, integrating phytohormone signalling and ageing (Sanmartin *et al.*, 2003; Barth *et al.*, 2006; Kotchoni *et al.*, 2009; Smirnov, 2011; Hanxia *et al.*, 2015; Bu *et al.*, 2016; Y. Yu *et al.*, 2019; Zhang *et al.*, 2020; Bulley *et al.*, 2021). As an essential micronutrient that humans have lost the ability to produce, AsA is required for key metabolic functions in humans and must be obtained from the diet, mainly from fruits and vegetables. Today, eating sufficient amounts of fruits and vegetables to consistently maintain optimum AsA concentrations is still a challenge for people in both developed and developing countries (Troesch *et al.*, 2012). Having higher plasma vitamin C concentrations is associated with positive health benefits such as reducing the risk of stroke, supporting the immune system, supporting cardiovascular health and reducing skin age appearance (Myint *et al.*, 2008;

Moser & Chun, 2016; Carr & Maggini, 2017; Pullar *et al.*, 2017). Considering the important role of AsA in human health, studies on the molecular mechanism underlying AsA accumulation in the fruit of some very high AsA-containing species, those with *c.* 500–3000 mg 100 g⁻¹ FW could help breeders increase the AsA content of crop plants in the future (Macknight *et al.*, 2017). Examples of these AsA superfruits include some species of the *Actinidia* genus (kiwifruit), *Rosa roxburghii* (chestnut rose), *Myrciaria dubia* (camu-camu) (Castro *et al.*, 2015), *Terminalia ferdinandiana* (Kakadu plum) and *Malpighia glabra* (acerola) (Badejo *et al.*, 2007). Indeed the high AsA trait carried by *A. eriantha* recently has been mapped to chromosome 26 and segregates as a large nonrecombinant portion of chromosome in *A. eriantha* × *A. deliciosa* × *A. chinensis* hybrids (McCallum *et al.*, 2019).

In plants, the accumulation of AsA is maintained in homeostasis through synthesis, recycling and degradation, as well as intra- and intercellular transport (Horemans *et al.*, 2000; Green & Fry,

2005a,b; Venkatesh & Park, 2014). It is well-known that AsA biosynthesis occurs through L-galactose, L-galacturonate and possibly L-myoinositol in certain instances (Wheeler *et al.*, 1998; Agius *et al.*, 2003; Lorence *et al.*, 2004; Bulley & Laing, 2016). The L-galactose pathway is the predominant route through which AsA accumulates in higher plants. All of the genes involved in this pathway have been characterized, and the flux-limiting steps in this pathway are the conversion of D-mannose-1-P to L-galactose-1-P, which is catalyzed in succession by the enzymes GDP-D-mannose pyrophosphorylase (*GMP*), GDP-D-mannose 3',5' epimerase (*GME*) and GDP-L-galactose-phosphorylase (*GGP*). Mounting evidence suggests that *GGP* is the key conduit for regulating AsA biosynthesis in plants (Dowdle *et al.*, 2007; Laing *et al.*, 2007, 2015; Linster *et al.*, 2007; Bulley *et al.*, 2009; Mellidou & Kanellis, 2017; Fenech *et al.*, 2021). Overexpressing the *GGP* gene consistently results in significant increases in AsA in a wide range of plant species (Macknight *et al.*, 2017). For example, up to a six-fold increase in AsA was achieved by overexpressing *GGP* in tomato (Bulley *et al.*, 2012).

The classical view of transcription factors (TFs) is that they regulate plant developmental and physiological processes by recognizing specific *cis*-acting elements and binding to promoters of target genes to control gene expression. To date, a number of TFs have been reported to be involved in AsA biosynthesis. These include the AP2 ethylene response factors ERF98 (Zhang *et al.*, 2012) and ABI4 (expressed only in roots) (Y. Yu *et al.*, 2019), the F-box protein ascorbic acid mannose pathway regulator 1 (AMR1) (Zhang *et al.*, 2009), the basic helix-loop-helix bHLH59 (Ye *et al.*, 2019), the HD-Zip family TF SIHZ24 (Hu *et al.*, 2016), and a novel ethylene-responsive TF (*BcERF070*) in cabbage (*Brassica rapa* ssp. *chinensis*) that binds to the dehydration-responsive elements (DREs) of seven target gene promoters to alter the AsA content (Yuan *et al.*, 2020). These factors, however, function differently and have relatively subtle effects (≤ 1.7 -fold) on the AsA content.

In the present study, we analyzed the AsA content in 48 *Actinidia* species and identified a new R1-MYB TF (AceMYBS1; MYB, myeloblastosis) from *A. eriantha*, whose fruit have a very high AsA content (500–1200 mg 100 g⁻¹ FW, > 10 times the AsA content of an orange fruit or > 50–120 times that of potato). This MYB appears to be a significant regulator of fruit AsA accumulation. We also identify a bZIP transcription factor AceGBF3 (GBF, G-box binding factor) which also can increase AsA and physically interacts with AceMYBS1. We also show that AceMYBS1, but not GBF3, is repressed by ABA which provides new insight about the molecular regulatory mechanism underlying AsA biosynthesis in kiwifruit.

Materials and Methods

Plant materials and growth conditions

Fruit samples were collected from field-grown plants in Hubei, China, during the 2016–2018 growing season. The L-ascorbic acid (AsA) content in the fruit of 48 *Actinidia* Lindl. species and one cross-population (*A. eriantha* Benth. \times *A. rufa* (Siebold &

Zucc.) Planch. ex Miq.) were measured during 2017–2019. Six kiwifruit taxa with significant variations in AsA content (> 150-fold), *A. eriantha* Benth., *A. latifolia* (Gardner & Champ.) Merr., *A. deliciosa* (A. Chev.) C.F. Liang and A.R. Ferguson, *A. chinensis* Planch., *A. rufa* (Siebold & Zucc.) Planch. ex Miq and *A. cylindrica* C.F. Liang, were selected to study the changes in AsA during fruit development. The media and protocols used were the same as those described previously (Z. Wang *et al.*, 2018). Tissue-cultured materials for both tobacco (*Nicotiana benthamiana* Domin) and kiwifruit (*A. eriantha* Benth.) were grown at 23–25°C under long-day conditions (16 h : 8 h, light : dark photoperiod). Transgenic and gene-edited plants were potted and grown in containment glasshouse-1 at the Wuhan Botanical Garden, Chinese Academy of Sciences, Hubei, China (14 h : 10 h, light : dark photoperiod, 18°C min, 30°C max). Samples collected from individual plants were considered to be biological replicates.

Illumina RNA-seq and transcriptome analysis

The detailed procedures of Illumina RNA-seq and transcriptome analysis are described in Supporting Information Methods S1, and the sequence data were uploaded to GenBank of NCBI (<https://www.ncbi.nlm.nih.gov/>) under accession nos. PRJNA771781 and PRJNA771785.

AsA measurement

Measurement of total AsA concentration was performed following the method as described previously, with minor modifications (Queval & Noctor, 2007; Li *et al.*, 2016; Liu *et al.*, 2021). Approximately 1.0 g of sample was harvested and immediately frozen in liquid nitrogen. The frozen samples were ground to a fine powder and extracted with 5 ml 0.1% metaphosphoric acid solution. After centrifuging at 8000 g for 10 min at 4°C, the supernatants and AsA standards (GWL8-54KE, China) were neutralized with NaOH and the final pH of all samples was between 5 and 6. The neutralized supernatants were pre-treated with 5 mM DL-dithiothreitol (DTT) for 30 min at room temperature. Next, the supernatants were filtered through a 0.22- μ m filter and 10.0 μ l of the supernatant was injected into Accela 1250 HPLC system (Thermo Fisher Scientific, Waltham, MA, USA) on a monomeric C18 column (Wondasil C18, Columns 5 μ m, 4.6 \times 150 mm; GL Sciences Inc., Shanghai, China) with a mobile phase of 0.1% metaphosphoric acid and acetonitrile (98 : 2, v/v). The flow rate of 0.5 ml min⁻¹ and injection volume of 10.0 μ l. The standard curve was drawn from the measured values of the AsA standard sample. The standard curves for AsA were generated as references to quantify the AsA content in the samples.

RNA extraction and quantitative reverse transcription (RT)-PCR analysis

Total RNA was isolated with an RNA Extraction Kit (Tiangen, Beijing, China) and the quantitative (q)RT-PCR analysis was

described previously (Z. Wang *et al.*, 2018); additional details are described in Methods S1 and primer sequences are listed in Table S1.

Phylogenetic analysis and tree construction

A phylogenetic tree for myeloblastosis (MYB)S1 was constructed using MEGA7.0 (Kumar *et al.*, 2016) software with kiwifruit and other species sequences retrieved from the kiwifruit database (<http://kiwifruitgenome.org/>) and the GenBank database (Table S2), respectively. Genetic distances were calculated using the Jukes–Cantor distance matrix and evolutionary relationships were inferred using the neighbour-joining method with 1000 bootstrap resampling.

Vector construction and kiwifruit transformation

The coding DNA sequences (CDS) of *AceGGP3*, *AceMYBS1* and *AceGBF3* were amplified from cDNA of *A. eriantha* and cloned into the overexpression vector POE-3Flag-DN (from Wuhan Botanical Garden laboratory) which has 35S promoter driven expression as well as resistance screening markers G418 (Geneticin; Invitrogen) and kanamycin to generate 35S::*AceGGP3*, 35S::*AceMYBS1*, 35S::*AcrMYBS1* and 35S::*AceGBF3*, respectively G-box binding factor (GBF).

The *AceGGP3* and *AceMYBS1* were edited by CRISPR/Cas9 as described previously (Z. Wang *et al.*, 2018). CRISPR RGEN Tools (http://www.rgenome.net/?tdsourcetag=s_pcqq_aiomsg) was used to select specific sgRNAs that targeted *AceGGP3* and *AceMYBS1*, respectively, and the sgRNAs were cloned into CRISPR/Cas9 vector to generate Cas9-*AceGGP3* and Cas9-*AceMYBS1* editing vectors. Using *Agrobacterium*-mediated transformation, the recombinant plasmids were transformed into the calli of *A. eriantha* following methods described previously (Akbaş *et al.*, 2009; X. Wang *et al.*, 2018; Z. Wang *et al.*, 2018). The primers used for vector construction and identification of transgenic lines are listed in Table S1.

Transient expression assay in kiwifruit and tobacco

The antisense viral vectors Anti-*AceGGP3*, Anti-*AceMYBS1* and Anti-*AceGBF3* were obtained by cloning the CDS of *AceGGP3*, *AceMYBS1* and *AceGBF3* into TRV2 vector (An *et al.*, 2019; M. Yu *et al.*, 2019) respectively. TRV1 vector was used as an auxiliary plasmid. The TRV1 and TRV2 vectors each were transformed into *Agrobacterium tumefaciens* GV3101 and mixed each other when injected or transfected into the fruits and calli of *A. eriantha*. The same method was used for transient overexpression experiments with 35S-driven *AceGGP3*, *AceMYBS1* and *AceGBF3* vectors in *A. eriantha* and *N. benthamiana* (tobacco) leaves.

Yeast one-hybrid assay

Yeast one-hybrid (Y1H) assay was performed as described previously (Lin *et al.*, 2007; Cheng *et al.*, 2021; Fu *et al.*, 2021). The promoter sequence of *AceGGP3* (2.6-kb; Table S2) were

amplified and inserted into the corresponding sites of the reporter plasmid pLacZi (Clontech; TaKaRa Bio Inc., Shiga, Japan) to generate *AceGGP3* pro::LacZ. The CDS of *AceMYBS1* were cloned separately into pJG4-5 vectors (Clontech; TaKaRa Bio Inc.) to construct pJG-*AceMYBS1*. The *NcoI*-cut *AceGGP3* pro::LacZ vector was co-transformed with pJG-*AceMYBS1* vector into yeast strain EGY48 using a high-efficiency yeast transformation method (Gietz & Schiestl, 2007), respectively. The p53::LacZ+pJG-p53 was used as positive control and the *AceGGP3*pro::LacZ add the pJG4-5 empty vector was the negative control. Transformants grew on SD/-Trp-Ura dropout medium. We selected transformants on the medium with 6.7 g l⁻¹ yeast nitrogen base, 20 g l⁻¹ Galactose, 10 g l⁻¹ Raffinose, 2 g l⁻¹ dropout mix-TRP-URA and 20 g l⁻¹ agar. After sterilization at 121°C for 15 min, 100 ml 10 × BU salt (contain 70 g l⁻¹ Na₂HPO₄·7H₂O and 30 g l⁻¹ NaH₂PO₄, pH = 7.0) and 0.08 mg ml⁻¹ X-gal were added for colorimetric screening. All of the yeast strains were incubated at 30°C for 3 d. The primers are listed in Table S1.

Yeast two-hybrid assay

Construction of a cDNA library of kiwifruit for yeast two-hybrid (Y2H) experiments was carried out by GeneCreate Biological Engineering Co. Ltd (Wuhan, China) using mRNA from the leaves and fruits. Details are described in Methods S1.

Transcriptional activation analysis

The full-length cDNA of *AceMYBS1* and *AceGBF3* were PCR-amplified and fused into pGBKT7 vector to generate two constructs (BD-*AceMYBS1* and BD-*AceGBF3*) which were transformed into the yeast strain AH109. The transcriptional activation analysis was performed as described previously (Geng & Liu, 2018).

Dual-luciferase assay

For the Dual-luciferase (Dual-LUC) assay, the full-length promoter of *AceGGP3* (2.6 kb, Notes S1) or their truncated fragments were cloned into the pGreen0800-Luc vector (Hellens *et al.*, 2005) to obtain reporters: *AceGGP3*pro-2660::LUC (*P*₂₆₆₀), *AceGGP3*pro-1106::LUC (*P*₁₁₀₆), *AceGGP3*pro-1606::LUC (*P*₁₆₀₆) and *AceGGP3*pro-2088::LUC (*P*₂₀₈₈). The 35S: *AceMYBS1* and 35S: *AceGBF3* were transformed into *A. tumefaciens* strain EHA105. Mixed effector and reporter construct carrying cultures (5:1, v/v, respectively) were co-infiltrated into 4-wk-old tobacco leaves as described previously (Gao *et al.*, 2020). After incubation for 2–3 d at 23°C, the promoter activities were determined by measuring Firefly Luciferase to Renilla Luciferase (LUC/REN) ratios using a Dual-luciferase Kit (TransGen, Beijing, China) with a Chemiluminescence Imaging System (Clinx, Shanghai, China).

Protein expression and electrophoretic mobility shift assay

The full-length *AceMYBS1* CDS was inserted into the pET32a vector (Novagen; Merck KGaA, Darmstadt, Germany)

containing 6xHis (fusion both in the N-terminal and C-terminal) and expressed using *E. coli* strain BL21 (TransGen) to produce recombinant AceMYBS1-His protein. An *E. coli* strain expressing 6xHis was used as a negative control. *Escherichia coli* was cultivated for 12 h at 16°C and then diluted 1 : 100 (v/v) into fresh medium and grown on for another 2–3 h at 37°C. When cell growth reached the logarithmic phase, IPTG was added to 0.5 mM final concentration and induced protein expression proceeded at 16°C for 10–12 h. The fusion protein was purified according to manufacturer instructions using Proteinso Ni-NAT Resin (TransGen). The oligonucleotide probes (Table S1) containing the AceMYBS1 binding sequences of AceGFP3, which was predicted by JASPAR2020 (<http://jaspar.genereg.net/>) were synthesized and labelled with biotin. Double-strand DNA probes were obtained by annealing two complementary oligonucleotides. The fusion protein AceMYBS1-His was mixed with probes and incubated at room temperature for 20 min. DNA gel mobility shift assay was performed using the EMSA Kit (Beyotime Biotechnology, Jiangsu, China) following the manufacturer's protocol.

Subcellular localization

The *AceMYBS1-YFP* or *AceGBF3-YFP* mixed with *NLS-mCherry-RFP* were co-infiltrated into tobacco leaves with infiltration buffer as described previously (Gao *et al.*, 2020). Fluorescence was observed 48 h post-infiltration by Confocal Microscopy (Leica TCS-SP8; excitation wavelength with YFP: 510 nm and RFP: 552 nm).

Bimolecular fluorescence complementation assay

The full-length *AceMYBS1* CDS was fused with C-terminal *YFP* (*C-YFP*), and *AceGBF3* was fused with N-terminal *YFP* (*N-YFP*). The recombinant vectors or control (empty vectors) were transformed into *A. tumefaciens* strain EHA105 and then co-transformed into onion epidermal cells with infiltration buffer (Zhu *et al.*, 2020). YFP fluorescence was detected by Confocal Microscopy (Leica TCS-SP8; excitation wavelength with YFP: 510 nm and DAPI: 488 nm) 48 h after infiltration.

Pull down

The full-length CDS of *AceGBF3* was cloned into pGEX-4T vector (GE Healthcare, Chicago, IL, USA) in which it is fused to glutathione-S-transferase (GST) sequence. The recombinant vectors were introduced into BL21 cells to produce *AceGBF3*-GST fusion protein, and expressed *AceGBF3*-GST and *AceMYBS1*-6xHis fusion protein was purified as described previously (Xu, 2020). Aliquots (20 µl) of *AceGBF3*-GST and *AceMYBS1*-His proteins were mixed with 1 ml binding buffer (50 mM Tris-HCl (pH = 7.5), 100 mM NaCl, 0.25% Triton-X100 (v/v), 35 mM β-Mercaptoethanol), then 50 µl Proteinso GST Resin or 50 µl Proteinso Ni-NAT Resin (TransGen) was added and the mixture was rotated at 4°C for 3–4 h. The samples were washed four times with binding buffer, with expressed GST or 6xHis used as negative

controls. 6xSDS protein loading buffer was added to samples (to 1 × final) and samples were denatured by boiling for 10 min before electrophoresis. After electrophoresis the gels analyzed by Western blot using anti-His (1 : 10 000 (v/v), Proteintech, 66005-1-lg) and anti-GST (1 : 10 000 (v/v), Proteintech, 66002-2-lg; both sourced from Wuhan Sanying, Wuhan, China) antibodies.

Bimolecular luminescence complementation assay

Bimolecular luminescence complementation (BiLC) assay was performed as described previously (Chen *et al.*, 2008). The full-length of *AceMYBS1* and *AceGBF3* CDS were inserted into pCambia1300-cLUC and pCambia1300-nLUC vector to create *AceMYBS1*-cLUC and *AceGBF3*-nLUC constructs, respectively. *Agrobacterium* cultures harbouring the different constructs were mixed at 1 : 1 (v/v) and co-transformed into tobacco leaves. Plants were incubated under dark for 12 h and then transferred to light conditions at 25°C for 48 h. Immediately before LUC activity observation, the transformed tobacco leaves were soaked in 0.15 mg ml⁻¹ D-Luciferin potassium (Coolaber, Beijing, China) for 2–3 min and images were captured using a Chemiluminescence Imaging System (Clinx, Shanghai, China).

ABA treatment

Different concentrations and durations of ABA treatment were used to investigate the effects of ABA on AsA biosynthesis in different materials of kiwifruit. First, ABA (GoldBio, St Louis, MO, USA) was added (0, 1, 2, 3, 5, 10 µM) to the callus media of *A. eriantha*, which were allowed to grow for 3 d under 16 h : 8 h, light : dark photoperiod at 25°C. Secondly, fruit from 80 d after flowering (DAF) *A. eriantha* on a vine or in *vitro* were sprayed with 20 µM ABA (or water for control) and then sampled at different times (0, 3, 5, 8, 10 d) thereafter.

Statistical analyses

One-way ANOVA was performed using SPSS v.20 (IBM Corp., Armonk, NY, USA), and Student's *t*-test was performed using GRAPHPAD 8.0 software. Significant differences were detected by Student's *t*-tests. In the figures, the following notations are used: *, *P* < 0.05; **, *P* < 0.01; and ***, *P* < 0.001. In figures, the different letters above the bars denote significance groupings (*P* < 0.05) as determined by ANOVA, the data represent the mean values, and error bars represent SD.

Accession numbers

The sequence information for this study was obtained from <http://kiwifruitgenome.org>, https://solgenomics.net/organism/Nicotiana_benthhamiana/genome, and <https://www.ncbi.nlm.nih.gov/> databases. Additionally, corresponding *Acc* gene models from *A. chinensis* (genotype Red5) are also referred to, and are the PS1.1.69.0 version gene models (Pilkington *et al.*, 2018). The GenBank accession numbers are listed in Table S2.

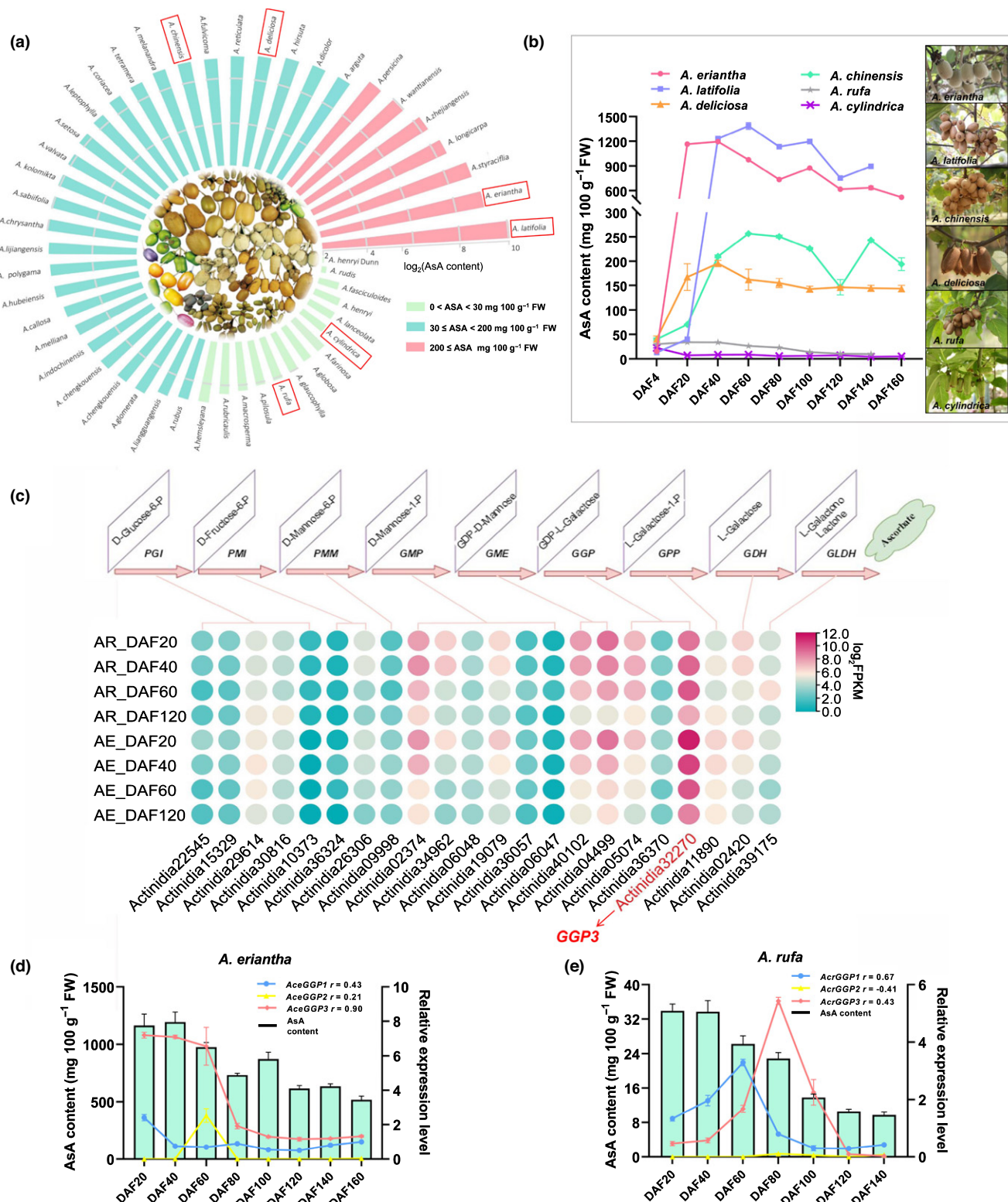


Fig. 1 The variation of fruit ascorbic acid (AsA) content and key gene expression analysis in *Actinidia* species. (a) The circle bar charts showing the AsA content (\log_2) of 48 different *Actinidia* species. The AsA content of the different species was classified into three classes: red bars, high AsA content ($\text{AsA} \geq 200 \text{ mg } 100 \text{ g}^{-1} \text{ FW}$); blue bars, medium AsA content ($30 \leq \text{AsA} < 200 \text{ mg } 100 \text{ g}^{-1} \text{ FW}$); and green bars, low AsA content ($\text{AsA} < 30 \text{ mg } 100 \text{ g}^{-1} \text{ FW}$). The red rectangles marked six *Actinidia* species with high (A. eriantha and A. latifolia), medium (A. chinensis and A. deliciosa) and low (A. rufa and A. cylindrica) fruit AsA concentration. (b) Changes of fruit AsA concentration in six species during growing season. (c) Circle heatmap showing the expression profile ($\log_2 \text{FPKM}$) of orthologous genes in the L-galactose pathway in the kiwifruit. The gene model associated with GGP3 is highlighted in red text. The correlation between the expression of GGP (GGP1, GGP2 and GGP3) and AsA content of (d) *A. eriantha* and (e) *A. rufa* in fruit developmental stage (every 20 d). Error bars indicate $\pm \text{SD}$ ($n = 3$).

Results

In order to determine the AsA variation among members of the *Actinidia* genus, the AsA content in the fruit of 48 species was determined by HPLC. The concentration varied 269-fold, ranging from 4.4 to 1185 mg 100 g⁻¹ FW (Fig. 1a). Species with low

(0–30 mg 100 g⁻¹ FW), moderate (31–200 mg 100 g⁻¹ FW) and high AsA (201–1200 mg 100 g⁻¹ FW) contents constituted 29.1%, 56.3% and 14.6% of the species, respectively. Changes in AsA contents during the growing season were determined in six *Actinidia* species representing low, moderate and high AsA concentrations (Fig. 1b). AsA content in *Actinidia* species with

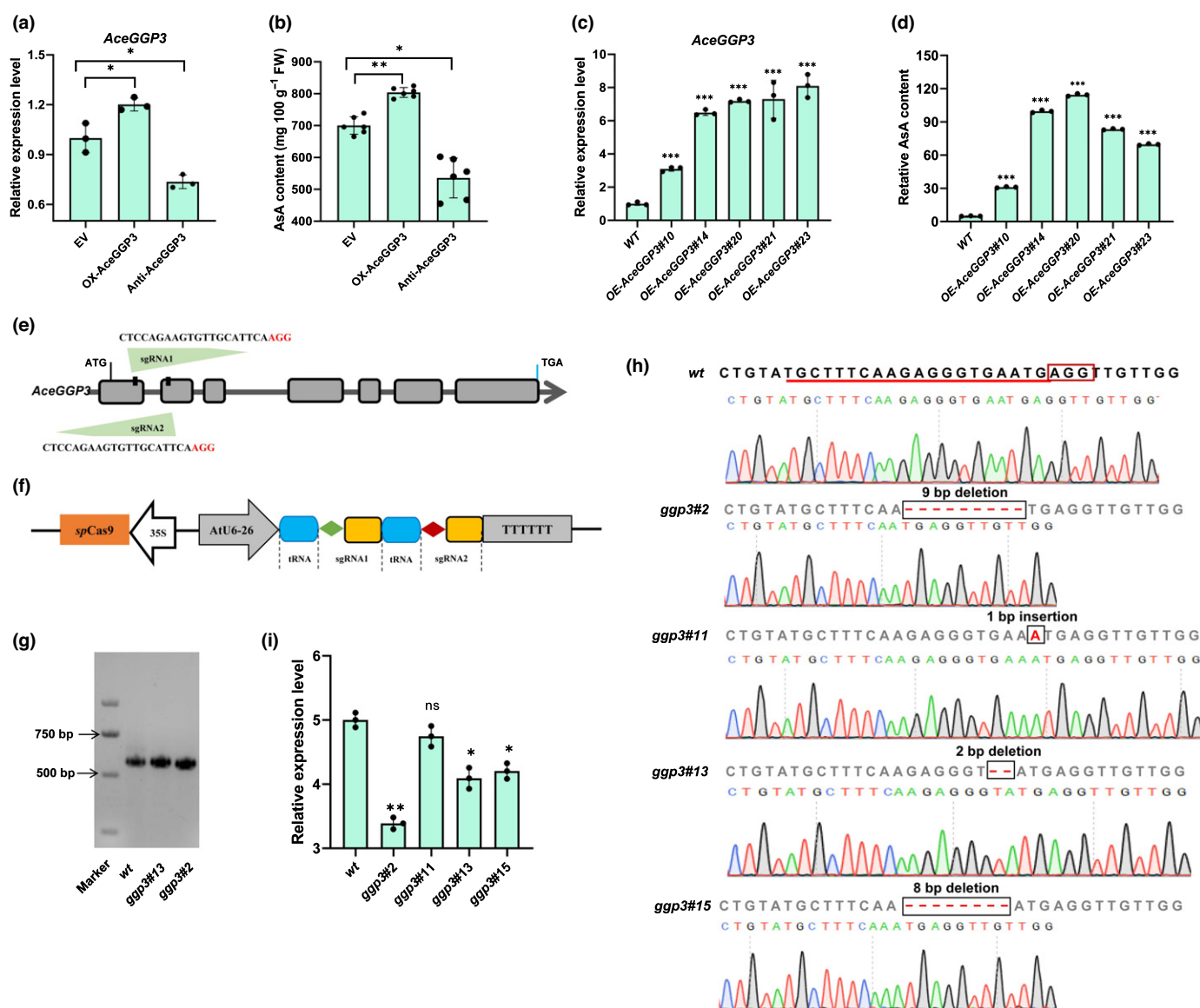


Fig. 2 Over- or knock-down expression of GDP-L-galactose-phosphorylase (*AceGGP3*) alters ascorbic acid (AsA) concentration in *Actinidia eriantha* fruit and calli. (a) Analysis of *AceGGP3* expression abundance and (b) AsA content of *A. eriantha* fruits with transiently expressed-*AceGGP3* 7 d after vector infiltration. EV, empty vector; OX-*AceGGP3*, *AceGGP3*-overexpression; TRV-*AceGGP3*, *AceGGP3*-antisense expression. Experiments were performed in six kiwifruits per genotype. (c) Quantitative reverse-transcription (qRT)-PCR analysis of *AceGGP3* and (d) relative AsA content in the five transgenic calli of *A. eriantha* with *AceGGP3*-overexpressed. WT, wild-type; OE-*GGP3*#10, OE-*GGP3*#14, OE-*GGP3*#20, OE-*GGP3*#21 and OE-*GGP3*#23 represent five different transgenic lines. (e) Schematic map of the sgRNA targeted sites on the exon regions of *AceGGP3*. Lines, intergenic region and introns; grey boxes, exons; red bases, PAM motifs (NGG). (f) Schematic diagram of the CRISPR/Cas9 vector and target site selection in the *AceGGP3* gene. Sequences of the two sgRNA: sgRNA1 (CTCCAGAAGTGTTCATTCAAGG) and sgRNA2 (TGCTTTCAAGAGGGTGAATGAGG). (g) Example of amplification using gene-specific primers, which identified the deletion in *AceGGP3* in lines *ggp3*#13 and *ggp3*#2, the wild-type (wt) as a control. (h) Sequencing results and chromatograms of the *AceGGP3* homozygous mutant lines from the T₁ generation. Red box, PAM motif; underlining, target sequence; dashes, deletions; and red letters, insertions. (i) Relative AsA content of *A. eriantha* calli in CRISPR/Cas9-induced mutants in the *AceGGP3*. *ggp3*#2, *ggp3*#11, *ggp3*#13 and *ggp3*#15 represent four gene editing lines (wt, wild-type). Each experiment of (c), (d) and (i) was performed in three replicates. All error bars denote \pm SD. Significant differences were detected by Student's *t*-test using GraphPad PRISM 8: *, $P < 0.05$; **, $P < 0.01$; ***, $P < 0.001$; ns, not significant. Black circles in bar charts represent individual data points.

high or moderate fruit AsA content accumulated AsA rapidly after fertilization, peaking at DAF40–60, before decreasing as the fruit progressed towards maturity, whereas that of low-AsA content species stayed low during the whole growing season (Fig. 1b). AsA biosynthesis during early fruit development appears to be the main reason for AsA accumulation among members of the *Actinidia* genus, and differences in AsA synthesis at this stage might constitute the main determinant of AsA variation among *Actinidia* species.

In order to identify potential AsA regulatory genes, transcriptome sequencing of fruit at 20, 40, 60 and 120 DAF

time points was performed for *A. eriantha* and *A. rufa*, whose fruit presented a >30-fold difference in AsA content. A total of 24 415 differentially expressed genes (DEGs) were identified by pairwise comparisons (Fig. S1a), and gene ontology (GO) enrichment analysis revealed that these DEGs were significantly enriched in biological processes related to the response to catalytic activity and biosynthetic processes (Fig. S1b). The transcript *Actinidia32270*, encoding *GGP3*, was identified in *A. eriantha* on the basis of the increased transcript abundance in the L-galactose pathway (Fig. 1c). Three *GGP* homologous genes were further subjected to

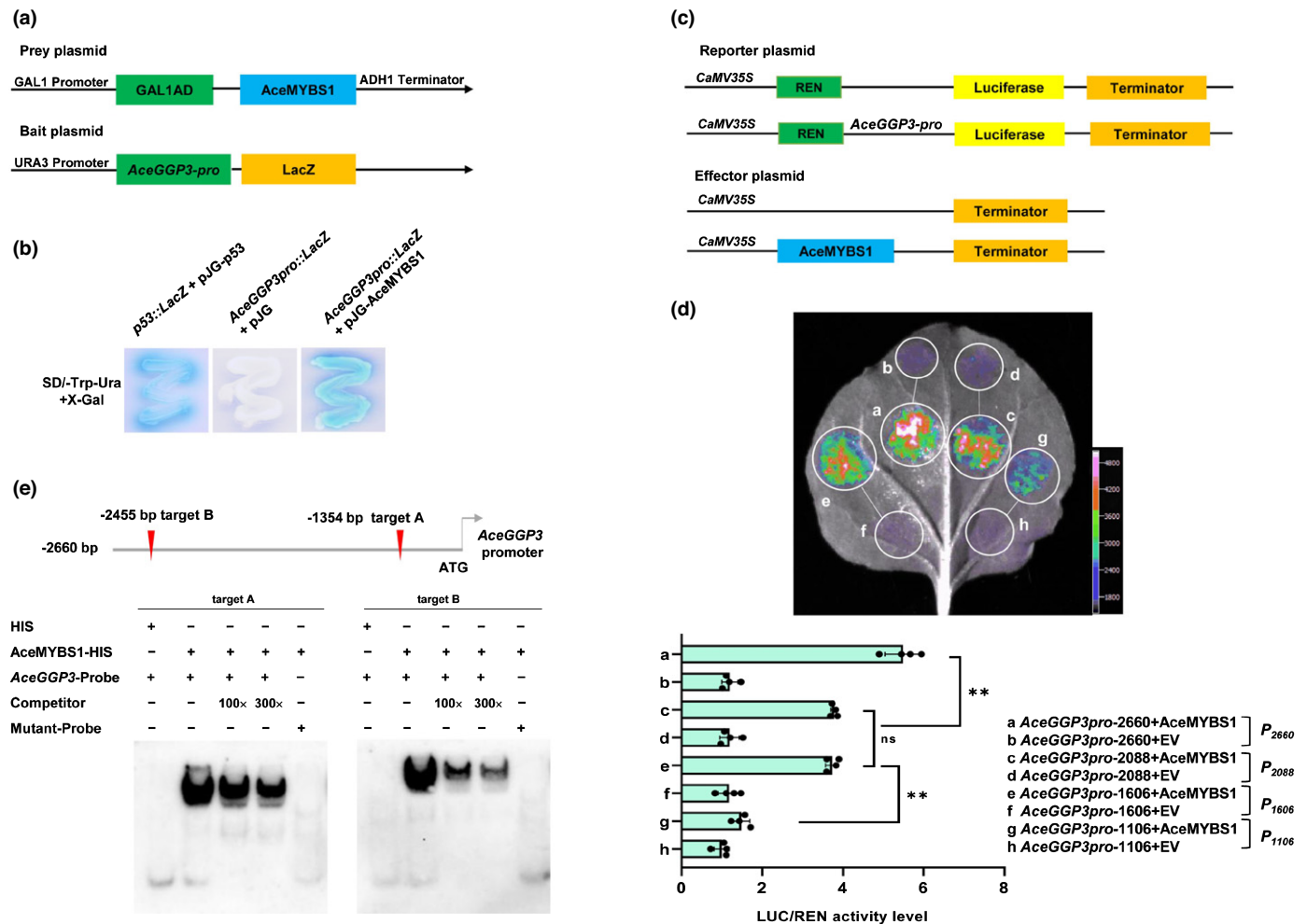


Fig. 3 The promoter of GDP-L-galactose-phosphorylase (*AceGGP3*) is the direct target of *AceMYBS1* (MYB, myeloblastosis). (a) Schematic diagram of the prey plasmid and bait plasmid in yeast one-hybrid (Y1H) assay. The promoter fragment of *AceGGP3* was cloned into the pLacZi vector to generate bait plasmid and the prey plasmid was generated by recombining the *AceMYBS1* gene into pJG4-5 vector. (b) Y1H assay showing the interaction between *AceMYBS1* and *AceGGP3* promoter (*AceGGP3pro::LacZ*). The yeast strains were grown on SD/-Trp/-Ura/+X-gal media for 3 d. The *p53::LacZ*+pJG-p53: positive control; *AceGGP3pro::LacZ*+pJG: negative control. (c) Schematic diagram of the reporter vector and effector vector. The promoter fragment of *AceGGP3* was cloned into the pGreenII 0800-LUC vector to generate the reporter construct. The effector was generated by recombining the *AceMYBS1* gene into an overexpression vector (POE-3×Flag-DN). (d) Dual-luciferase (LUC) assay in *Nicotiana benthamiana* leaves showing that *AceMYBS1* activates transcription of different-length fragments of *AceGGP3* promoters (P_{2660} , P_{2088} , P_{1606} , P_{1106}). The empty vector is the control. Representative photographs were taken (above), and LUC/Renilla Luciferase (REN) activity detection to verify that *AceMYBS1* activates the transcription of *AceGGP3* (below). Error bars: \pm SD. Significant differences were detected by Student's *t*-test: **, $P < 0.01$; ns, not significant. Black circles in bar chart represent individual data points. (e) Position of two *AceMYBS1* predicted binding targets on the *AceGGP3* promoter and electrophoretic mobility shift assay (EMSA) showing the binding of *AceMYBS1* to the *AceGGP3* promoter. The unlabelled probes were used as competitors. 100× and 300× represent the rates of the competitor. The target A probes 5'-TAATTAATAGATAAGAAAAGAGAAAAAGG-3' were replaced with 5'-TAATTAATAAAAAAAAAAAGAGAAAAAGG-3'; target B probes 5'-AAATAAGGGCAATCTTATCATTATGTCAA-3' were replaced with 5'-AAATAAGGGCAAAAAAAAAATTATGTCAA-3'. All the probe sequences are listed in Supporting Information Table S1.

qRT-PCR and correlation analysis of AsA contents in the fruits of *A. eriantha*, *A. rufa* and their hybrids at different developmental stages (Figs 1d,e, S2). *GGP3* in *A. eriantha* (*AceGGP3*) was most highly expressed and positively correlated with the high AsA content in the fruits (Figs 1d,e, S2). Furthermore, *GGP3* expression also was correlated to AsA concentration in the *A. eriantha* × *A. rufa* hybrid (Fig. S3a,b), and the expression of *AceGGP3* allele derived from *A. eriantha* was significantly higher than the expression of the *A. rufa*-derived allele *AcrGGP3* (Fig. S3c).

AceGGP3 overexpression leads to a sharp accumulation of AsA in kiwifruit

Transient expression assay experiments were performed to confirm the function of *AceGGP3* in AsA accumulation using 35S-driven *AceGGP3* overexpression and silencing constructs in on-vine kiwifruit and calli in tissue culture. At 7 d postinfiltration *AceGGP3* expression and AsA content were slightly higher than in the control fruit (Fig. 2a,b). Moreover, silencing of *AceGGP3* in fruiting plants led to a c. 24.0% decrease in AsA compared with that in fruit infiltrated with bacteria harbouring empty vectors (Fig. 2b). In transient assays of *A. eriantha* calli, overexpression of *AceGGP3* significantly increased the AsA content (Fig. S4). It is likely that the small AsA increase in transient fruit expression is a consequence of challenges with performing transient expression in on-vine fruit with potentially inconsistent results. Callus tissue showed much higher increases in AsA.

In order to further analyze *AceGGP3* function, transgenic kiwifruit lines were generated by *Agrobacterium* transformation of calli. Five independent transgenic lines of *A. eriantha* overexpressing *AceGGP3* were obtained. Compared with wild-type (WT) plants, the transgenic plants exhibited varying degrees of *AceGGP3* gene expression, from 3.1- to 8.1-fold (Fig. 2c), and AsA contents increased by 6.3-, 20.0-, 22.7-, 16.7- and 14.1-fold, respectively (Fig. 2d). *AceGGP3* then was mutated in kiwifruit via the CRISPR/Cas9 system, and the two targeted sites were located on the first and second exons of *AceGGP3* (Fig. 2e, f). In total, four G418-resistant lines containing three types of homozygous mutant *AceGGP3* genes (*ggp3#2*, a 9-bp deletion; *ggp3#11* and *#15*, an 8-bp deletion; *ggp3#13*, a 2-bp insertion; Fig. 2g,h) were selected. Three mutations resulted in frameshift mutations or amino acid deletions that induced premature termination or truncation of the predicted protein, causing a loss of the *AceGGP3* gene function. The AsA content in the fruit of the *ggp3* mutants decreased by 32.2%, 5.11% (not statistically significant), 18.2% and 15.9% compared with that of the WT (Fig. 2i). The 1-bp insertion in *ggp3#11* was predicted to cause a non-sense frameshift but AsA amounts remained effectively unchanged. However, a scan of open reading frames (ORFs) in this mutated CDS showed that translation initiation from the fourth ATG codon downstream would produce a truncated version of *GGP* missing 53 amino acids from the N-terminus, and the unchanged AsA content in *ggp3#11* suggests that this variant has functional *GGP* activity. Collectively, the results show that

up- or downregulated expression of *AceGGP3* has a large effect on AsA accumulation in *A. eriantha*.

AceMYBS1 acts as a transcriptional activator of *AceGGP3*

Through transcriptome analysis a TF, Actinidia31027 (*Actinidia chinensis* (Hongyang) protein v3; Acc18653.1: *Actinidia chinensis* Red5 Genome, LG16-18681898 ... 18 684 251; DTZ79_16g09490: *Actinidia eriantha* White Genome, Chr16: 11 608 690 ... 11 611 254), whose expression was strongly correlated with *Actinidia32270* (*GGP3*) expression, was identified (Table S3), and qRT-PCR analysis also showed that its expression was highly correlated with both *AceGGP3* expression and AsA content in *A. eriantha* (Fig. S5a,b). A phylogenetic tree comprising the sequences of amino acids of Actinidia31027 and MYBs of other plant species showed that Actinidia31027 was most closely related to TwMYBS1 from *Tripterygium wilfordii*, as they shared 86% amino acid sequence identity, whereas it was most distant to CcMYB5 from *Citrus clementina* (Fig. S5c). We thus designated this protein as AceMYBS1. Multiple alignments performed on the SMART website (<http://smart.embl-heidelberg.de/>) (Schultz *et al.*, 1998; Letunic *et al.*, 2020) showed that Actinidia31027 contains two SANT/MYB regions. A SANT domain is a protein domain that allows many chromatin remodelling proteins to interact with histones (Boyer *et al.*, 2002, 2004), and because SANT domains share many similarities with MYB DNA binding domains, they are often conflated. SANT and MYB domains can be distinguished by the predicted isoelectric point (pI) of the domain peptide, with histone-interacting SANT domains having acidic pIs, and MYB DNA binding domains having basic pI (Ko *et al.*, 2008). The N-terminal SANT of Actinidia31027 has a predicted acidic pI and the second SANT/MYB region has a predicted basic pI (Fig. S6). Therefore, this predicts that AceMYBS1 has one histone-interacting domain at its N-terminus side and a MYB DNA-binding domain in the middle of the protein (Fig. S6).

In order to reveal the mechanism by which *AceGGP3* is regulated by AceMYBS1, we first conducted a Y1H assay. All of the yeast cells grew well on SD/-Trp/-Ura media, whereas only the positive control and bait vector *AceGGP3pro::LacZ* co-transformed with the prey vector pJG-AceMYBS1 had blue cells on media supplemented with X-gal showing AceMYBS1-promoted expression of *LacZ* driven by the *AceGGP3* promoter (Fig. 3a,b). The AceMYBS1 and *AceGGP3* promoter co-transfected tobacco also had a much higher relative LUC/REN ratio than control in a Dual-LUC assay supporting interaction (Fig. S7).

The *cis*-elements of *MYBS1* were predicted by JASPAR 2020 (Fornes *et al.*, 2019). Among many predicted *MYBS1 cis-elements*, two main *cis*-elements were identified within the *AceGGP3* promoter (−2455 bp, TCTTATC; −1534 bp, TCTTATC) (Fig. S8a). Four 5'-truncated *AceGGP3* promoters (designated *P*₁₁₀₆, *P*₁₆₀₆, *P*₂₀₈₈ and *P*₂₆₆₀) were amplified from *A. eriantha*, and the transcriptional activity was assessed with a Dual-LUC reporter system (Fig. 3c,d). The activities of *P*₁₆₀₆ and *P*₂₆₆₀ were

higher than those of P_{1106} and P_{2088} , indicating that *cis*-elements are likely to be located between positions -1106 – 1606 bp and -2088 – 2660 bp, which is the same interval as the predicted position. To verify the binding specificity of AceMYBS1 to these motifs, we carried out electrophoretic mobility shift assays

(EMSAs) and found that AceMYBS1-HIS fusion proteins (Fig. S8b) could bind DNA probes containing the motifs, whereas nonlabelled competing probes effectively reduced the binding ability of AceMYBS1 in a dose-dependent manner, and mutation of the core sequence abolished the binding (Fig. 3e).

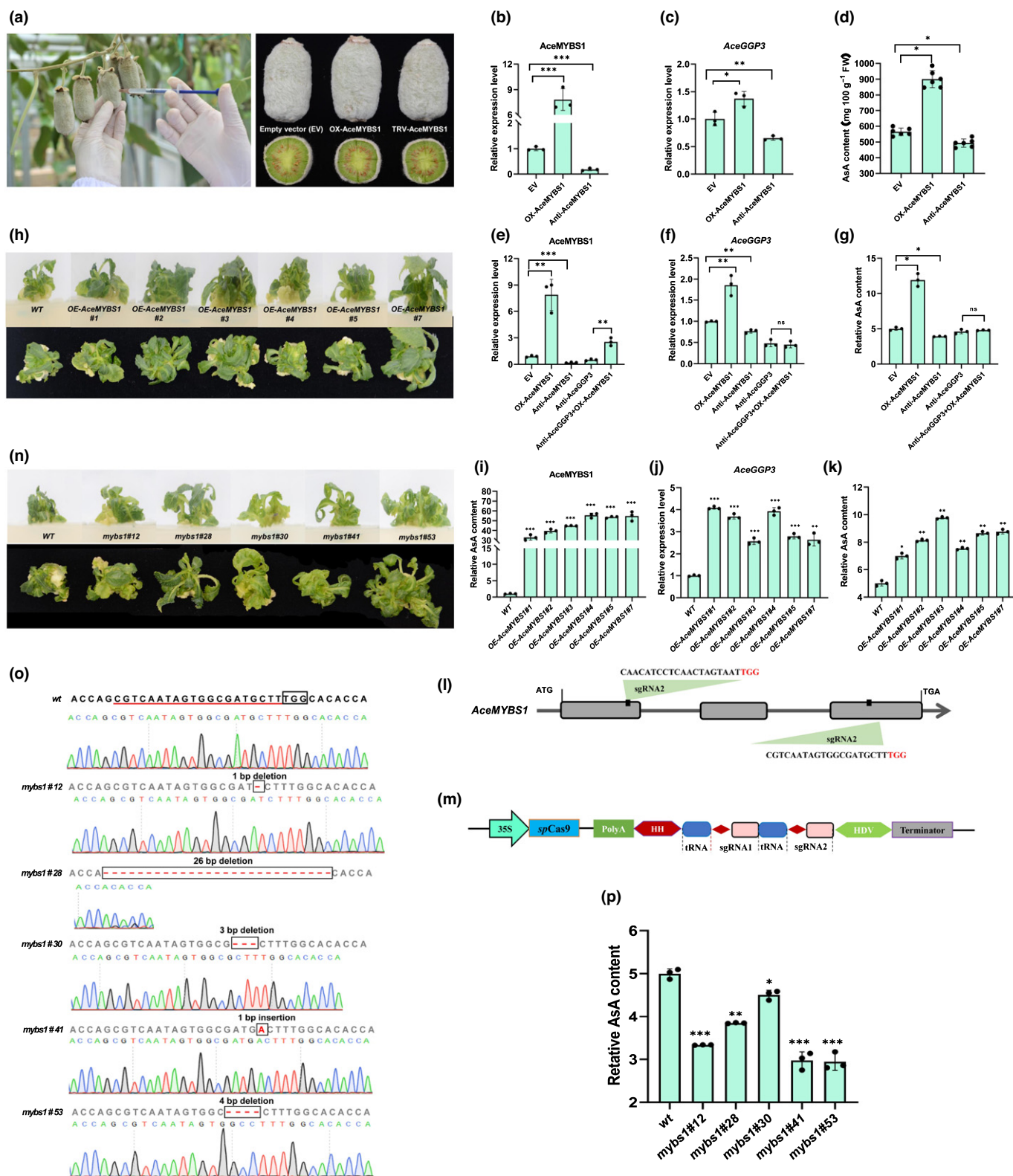


Fig. 4 AceMYBS1 positively regulates ascorbic acid (AsA) content in *Actinidia eriantha* fruit and calli (MYB, myeloblastosis). (a) Transient expression assay performed in on-tree fruits of *A. eriantha* at 80 d after flowering (80DAF). Quantitative reverse-transcription (qRT)-PCR analysis of (b) AceMYBS1, and (c) AceGGP3 and (d) AsA content of *A. eriantha* fruits with transient expressed-AceMYBS1 7 d after vector infiltration. EV, empty vector; OX-AceMYBS1, AceMYBS1-overexpression; Anti-AceMYBS1, AceMYBS1-antisense expression. Experiments were performed in six kiwifruits per genotype. qRT-PCR analysis expression of (e) AceMYBS1 and (f) AceGGP3 transcripts, and (g) relative AsA content of AceMYBS1 and AceGGP3 transient expressed in *A. eriantha* calli. Anti-AceGGP3: AceGGP3-antisense expression; Anti-AceGGP3+OX-AceMYBS1: overexpressed AceMYBS1 in Anti-AceGGP3 background. (h) Wild-type (WT) and six AceMYBS1-overexpression transgenic kiwifruit (*A. eriantha*) lines in tissue culture. OE-AceMYBS1#1, OE-AceMYBS1#2, OE-AceMYBS1#3, OE-AceMYBS1#4, OE-AceMYBS1#5 and OE-AceMYBS1#7 represent six different transgenic lines respectively. qRT-PCR analysis of (i) AceMYBS1 and (j) AceGGP3 in transgenic kiwifruit lines in (h). (k) Relative AsA content of AceMYBS1-overexpression transgenic kiwifruit calli in (h). (l) Schematic map of the sgRNA targeted site on the genomic regions of AceMYBS1. Lines, intergenic region and introns; grey boxes, exons; and red bases, PAM motifs (NGG). (m) Schematic diagram of the CRISPR/Cas9 vector. Sequences of sgRNA: sgRNA1 (CGTCAATAGTGCGATGCTTTGG) and sgRNA2 (CAACATCCTCAACTAGTAATTGG). (n) Phenotype of WT and five AceMYBS1-editing mutant lines: *mybs1#12*, *mybs1#28*, *mybs1#30*, *mybs1#41* and *mybs1#53*. (o) Sequencing results and chromatograms of the AceMYBS1 homozygous mutant lines from the T₁ generation with PAM motif boxed. (p) Relative AsA content of AceMYBS1-edited kiwifruit calli (l); note each experiment of (e–g), (i–k) and (p) were performed in three replicates (wt, wild-type). All of the above error bars denote standard deviation (\pm SD). Significant differences to WT were detected by Student's *t*-test using GraphPad PRISM 8: *, $P < 0.05$; **, $P < 0.01$; ***, $P < 0.001$. Black circles in bar charts represent individual data points.

These results indicate that AceMYBS1 binds directly to the *AceGGP3* promoter and acts as a transcriptional activator of *AceGGP3*.

In order to explore the AceMYBS1 expression profiles of *A. eriantha*, qRT-PCR was performed to assess transcript accumulation in the fruit. Consistent with AsA content, AceMYBS1 was highly expressed in the early fruit development stage and was positively correlated with the expression of *AceGGP3* (Fig. S5a,b). A transient expression assay in *A. eriantha* fruit (Fig. 4a–d) confirmed that the overexpression of AceMYBS1 increased the expression of *AceGGP3* by 1.4-fold (Fig. 4b,c), leading to a 1.7-fold increase in the AsA content in the fruit (Fig. 4d). By contrast, the expression level of *AceGGP3* in the Anti-AceMYBS1 fruit decreased by 30% (Fig. 4b,c). As in fruit, overexpression of AceMYBS1 in *A. eriantha* calli equally led to increased expression of *AceGGP3* (1.8-fold) and content of AsA (2.36-fold), and compared with empty vector-infected calli, Anti-AceMYBS1-infected calli exhibited significantly decreased *AceGGP3* expression and AsA content (Fig. 4e–g). When *AceGGP3* was suppressed by Anti-AceGGP3, AsA content did not increase, even when AceMYBS1 was overexpressed in *A. eriantha* calli and transgenic lines (Fig. 4f,g), suggesting that AceMYBS1 is an upstream regulatory gene of *AceGGP3*.

In order to gain further understanding of the regulatory roles of AceMYBS1, six stable overexpression transgenic kiwifruit lines were generated (Fig. 4h–k). qRT-PCR confirmed that the six independent transgenic lines accumulated high levels of AceMYBS1 transcripts (> 32- to 55-fold; Fig. 4i), which in turn increased the expression levels of *AceGGP3* by 2.5- to 4-fold (Fig. 4j). AsA content increased by 1.4-, 1.6-, 2.0-, 1.5-, 1.7- and 1.8-fold in comparison to those of controls, respectively (Fig. 4k). Using the CRISPR/Cas9 system, we further mutated AceMYBS1 in *A. eriantha* (Fig. 4l–p). The two targeted sites were located within the first and third exons (Fig. 4l,m). In total, five independent AceMYBS1 mutants (*mybs1#12*, a 1-bp deletion; *mybs1#28*, a 26-bp deletion; *mybs1#30*, a 3-bp deletion; *mybs1#41*, a 1-bp insertion; *mybs1#53*, a 4-bp deletion) (Fig. 4o) were identified. The AsA contents of the AceMYBS1-edited lines decreased by 33.2%, 23.1%, 9.8%, 40.4% and 40.0%, respectively (Fig. 4p). For *mybs1#30* which only had a 9.8% reduction in AsA content, while the 3 bp deletion of ATG was not in-frame, the effect was

only slight because the result was effectively synonymous owing to degeneracy, and the only difference to WT was the loss of an aspartic acid at position 205 (just over 20 amino acids downstream from MYB DNA binding domain). Taken together, these findings support that AceMYBS1 is a positive factor that modulates AsA synthesis.

AceGBF3 functions additively with AceMYBS1 to upregulate the expression of *AceGGP3* and increase the synthesis of AsA in kiwifruit

In order to further study the function of AceMYBS1 a Y2H screen was conducted to identify AceMYBS1-interacting proteins. A total of 85 yeast transformants were screened, and eight positive clones were identified as containing the same cDNA as its full-length sequence. This sequence encodes a bZIP protein (*Actinidia27344*), whose expression also correlated with *AceGGP3* expression (Table S3); this protein then was designated as AceGBF3 based on bioinformatic analysis (Figs 5a,b, S9). Further domain mapping analysis revealed that the N-terminal region (AceGBF3-N, amino acids 1–151) but not the C-terminal half (AceGBF3-C, amino acids 152–300) of AceGBF3 interacted with AceMYBS1 (Fig. S10a). An additional transcriptional activity assay was performed. Yeast cells transformed with BD-AceMYBS1 or BD-AceGBF3 but not the empty pGBKT7 vector grew normally and turned blue on SD/-T/-H/-A/+X- α -Gal medium (Fig. S10b). Subcellular localization assays were performed in tobacco leaves transformed with a nuclear marker to visualize the subcellular locations of AceMYBS1 and AceGBF3 and fluorescence of the AceMYBS1 and AceGBF3-fused yellow fluorescent protein (YFP) proteins was detected only in the nucleus and perfectly merged with nuclear markers (Fig. S11).

In order to further explore potential interactions between the AceGBF3 and AceMYBS1 proteins, three different methods were employed. First, a BiFC experiment was selected as a method for an *in vivo* assay using a cell biology approach. AceMYBS1 and AceGBF3 proteins were fused to the C-terminus of YFP (AceMYBS1-CYFP) and the N-terminus of YFP (AceGBF3-NYFP), respectively, and then transiently transformed into onion epidermal cells. The YFP signal localized to the nucleus showing close interaction between AceMYBS1 and

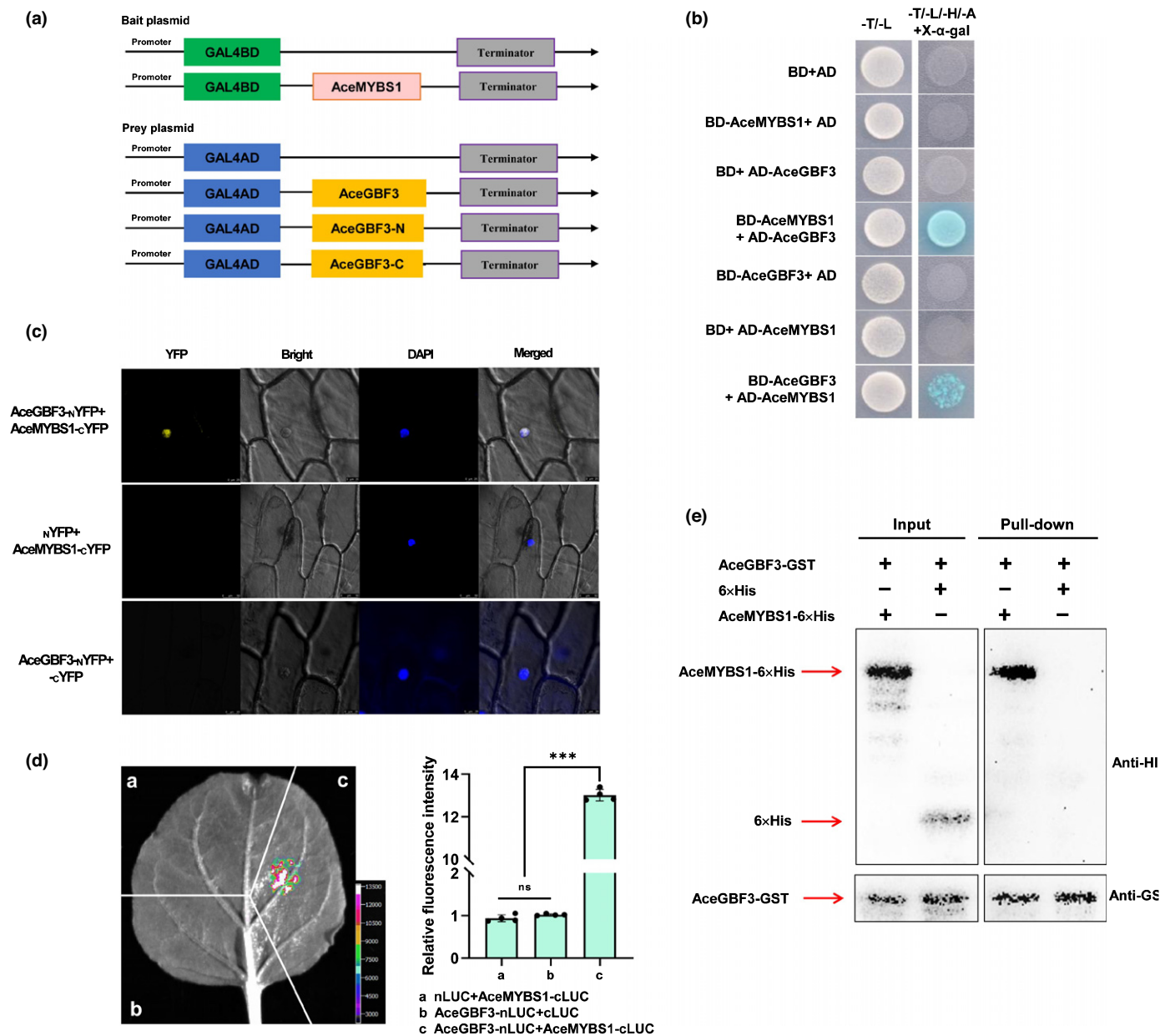


Fig. 5 AceMYBS1 interacts with AceGBF3 (GBF, G-box binding factor; MYB, myeloblastosis). (a) Schematic diagram of yeast two-hybrid assay. (b) Transformed yeast cells were grown on SD/-Trp/-Leu (-T-L) and SD/-Trp/-Leu/-His/-Ade/+X- α -gal (-T-L-H-A/+X- α -gal) media with empty pGADT7 (AD) used as negative control. (c) Bimolecular fluorescence complementation (BiFC) analysis of the interaction between AceMYBS1 and AceGBF3 in onion (*Allium cepa*) epidermal cells. Blue and yellow fluorescence represent DAPI and YFP signal, respectively, and the empty $_N$ YFP or $_C$ YFP vector was used as negative control. (d) Bimolecular luminescence complementation (BiLC) assay demonstrating that AceMYBS1 interacts with AceGBF3 *in vivo* in transient expression assay in *Nicotiana benthamiana* leaf where *Agrobacterium* cultures containing the respective recombinant plasmids were combined at 1 : 1 (v/v). Left, representative picture; right, measured relative fluorescence intensity. Error bars \pm SD; significant differences were detected by Student's *t*-test: ***, $P < 0.001$; ns, not significant. Black circles in bar chart represent individual data points. (e) *In vitro* pull-down assay where AceGBF3-GST protein was incubated with immobilized AceMYBS1-6 \times His or 6 \times His protein, and immunoprecipitated fractions were detected by Anti-GST antibody (GST, glutathione-S-transferase).

AceGBF3 as well as nuclear localization (Fig. 5c). To confirm this interaction, AceMYBS1 was fused to the C-terminal half of *LUC* (AceMYBS1-*cLUC*) and AceGBF3 was fused to the N-terminal half of *LUC* (AceGBF3-*nLUC*) and the constructs were transiently expressed in tobacco leaves (*N. benthamiana*). Only leaves co-transformed with AceMYBS1-*cLUC* and AceGBF3-*nLUC* produced a strong LUC signal (Fig. 5d). Finally, AceMYBS1-

AceGBF3 physical interactions were confirmed via an *in vitro* pull-down assay using recombinant purified proteins. The AceGBF3-GST fusion protein (Fig. S8b) was precipitated with AceMYBS1-6 \times His but not with 6 \times His alone when GST resin was used (Fig. 5e).

In order to test the hypothesis that AceGBF3 and AceMYBS1 co-regulate AsA synthesis, we performed Dual-LUC,

overexpression and virus-induced gene silencing experiments. These showed that AceMYBS1 and AceMYBS1 plus AceGBF3 but not AceGBF3 alone were capable of inducing the expression of *AceGGP3* (which increased by 3.74- and 6.67-fold, respectively; Fig. 6a). Transient overexpression of AceGBF3 in different plant materials, including kiwifruit (Fig. 6b–d), calli (Fig. 6e–g) and tobacco leaves (Fig. S12), consistently promoted the accumulation of AsA (Figs 6b–g, S12). Furthermore, co-overexpression of AceGBF3 together with AceMYBS1 promoted the accumulation of AsA additively (Figs 6h–k, S13). When AceMYBS1 was silenced in *A. eriantha* fruit, both the expression level of *AceGGP3* and the content of AsA were notably reduced or unchanged, regardless of whether AceGBF3 was overexpressed or suppressed, confirming that AceGBF3 has to interact with AceMYBS1 to upregulate the transcription of *AceGGP3* (Fig. 6h–k). Moreover, five transgenic *A. eriantha* lines constitutively overexpressing AceGBF3 were generated (Fig. 6l), and their *AceGGP3* transcript levels (Fig. 6m) and AsA contents increased by 2.11–3.38-fold and 1.22–1.78-fold (Fig. 6n), respectively, consistent with previous results. The average AsA content in transgenic calli (which was *c.* two-fold higher than that in WT calli) of the AceGBF3 and AceMYBS1 co-expression lines was significantly higher than those in the calli of the AceGBF3 (1.4-fold) and AceMYBS1 (1.6-fold) lines alone (Fig. 6o–r). Taken together, these results show that AceGBF3 interacts with AceMYBS1 to co-regulate *AceGGP3* expression to form an AceGBF3-AceMYBS1-*AceGGP3* regulatory network involved in the synthesis and metabolism of AsA in kiwifruit.

ABA inhibits the AceGBF3-AceMYBS1-*AceGGP3*-mediated regulation of AsA synthesis networks via AceMYBS1

Accumulating evidence has demonstrated that ABA plays a role in the biosynthesis of AsA (Y. Yu *et al.*, 2019; Kakan *et al.*, 2021). To determine the effects of ABA on the AceGBF3-AceMYBS1-*AceGGP3* regulatory network, calli were treated with ABA (0, 1, 2, 3, 5 and 10 μ M) and this showed that ABA inhibits the synthesis of AsA, especially at 2 μ M (Fig. S14). A Dual-LUC assay was used to test how ABA influences the interaction of AceMYBS1 and AceGBF3. Given that AceMYBS1 and AceGBF3 coexist with the *AceGGP3* promoter, the LUC/REN ratio was higher than that of the control when AceMYBS1 was co-expressed with the *AceGGP3* promoter-LUC, and it sharply declined when 2 μ M ABA was added (Fig. 7a). Consistent with these findings, the fluorescence intensity of activated AceMYBS1-C-LUC and AceGBF3-N-LUC in the BiLC assay was notably reduced in response to ABA (Fig. 7b).

In order to determine which TFs are affected by ABA, we sprayed *A. eriantha* fruit on the vine with 20 μ M ABA, and the results showed that ABA inhibited the synthesis of AsA especially on days 3 and 10 after treatment (Fig. 7c). qRT-PCR analysis showed that *AceMYBS1*, but not *AceGBF3* expression, was repressed by ABA treatment (Fig. 7d,e). Moreover, the fruit of *A. eriantha* were sprayed with ABA *in vitro* (Fig. 7f–h) and consistent with previous results, ABA inhibited the AsA synthesis and expression of *AceMYBS1*, and there

was little change in *AceGBF3* expression (Fig. 7f–h). AceMYBS1-overexpression lines treated with ABA showed a decrease in AsA concentration and expression of *AceGGP3* (Fig. 7i,j), whereas in ABA treated gene-edited lines of *mybs1*, AsA contents lines did not change (Fig. 7k). In particular, the expression of *AceGGP3* was unaffected by ABA if the *AceMYBS1* TF was mutated (Fig. 7l). The above results were confirmed in a transient experiment involving *A. eriantha* calli, and no significant changes in AsA content were observed after ABA treatment as long as *AceMYBS1* was silenced (Fig. S15). These data imply that ABA represses AsA content mainly by repressing the expression of *AceMYBS1*.

Discussion

L-ascorbic acid (AsA, vitamin C) is an essential human micronutrient obtained predominately from plants, especially from AsA-rich fruits and/or vegetative parts (Mittler, 2002; Gill & Tuteja, 2010; De Tullio, 2012). Kiwifruit are excellent sources of AsA, with ≤ 10 -fold higher content than that in apple and pear fruits, placing kiwifruit in the top echelon of available dietary sources of vitamin C. However, the AsA content in the fruits of *Actinidia* species varies considerably: from as low as 4–5 mg 100 g⁻¹ FW in the fruit of *A. henryi* to astonishingly high amounts (671–2140 mg 100 g⁻¹ FW) in *A. latifolia* (Huang *et al.*, 2004; Du *et al.*, 2009; Latocha *et al.*, 2010) (Fig. 1a). Our research indicates that the extreme variation in AsA contents among *Actinidia* species is probably due to the level of AsA synthesis activity during early fruit development, especially within the first 60 d (Figs 1b–e, S2). Within this window the expression of GDP-D-mannose pyrophosphorylase (*GMP*), GDP-D-mannose 3',5' epimerase (*GME*) and *AceGGP3* (GDP-L-galactose-phosphorylase) positively correlated with AsA accumulation, and expression of *GGP3* was more strongly correlated with AsA content in *A. eriantha* than in *A. rufa* (Figs 1c–e, S2). Thus, genotypes with higher expression of *GGP* are likely to have higher AsA content, and this is supported by conclusions from previous studies in kiwifruit and other species (Laing *et al.*, 2007; Bulley *et al.*, 2009, 2012; Zhou *et al.*, 2012; Li *et al.*, 2013b; Zhang *et al.*, 2015; Mellidou & Kanellis, 2017; Fenech *et al.*, 2021).

AceMYBS1 activates the transcription of *AceGGP3* to modulate the AsA content in *A. eriantha*

Transcription factors (TFs) are a group of regulators that play crucial roles in many biological and developmental processes in plants by regulating spatiotemporal gene expression through recognition of specific DNA sequences in promoters (Mitsuda & Ohme-Takagi, 2009). Although the biosynthesis of AsA is most responsive to *GGP* activity in kiwifruit, knowledge about the mechanisms involved in the regulation of *GGP* transcription is fairly limited. The TFs SIHZ24 (Hu *et al.*, 2016) and SINFYA10 (Chen *et al.*, 2020) bind to *VTCL*, *GGP* and *GME* to promote or reduce AsA synthesis. More recently, a kiwifruit ethylene response factor *AcERF91* has been found to increase the

expression of *AceGGP3* (Chen *et al.*, 2021), but overexpression of this gene produced only a modest increase in AsA. In this study we identified a kiwifruit 1R-subtype myeloblastosis (MYB) TF whose expression correlates with *AceGGP3* expression and AsA

content, with overexpression leading to larger increases in AsA. MYBS1 governs the sugar- and gibberellin-mediated regulation of α -amylase gene expression in cereals and rice (Lu *et al.*, 2002; Hong *et al.*, 2012), but plays an opposite role in sugar and ABA

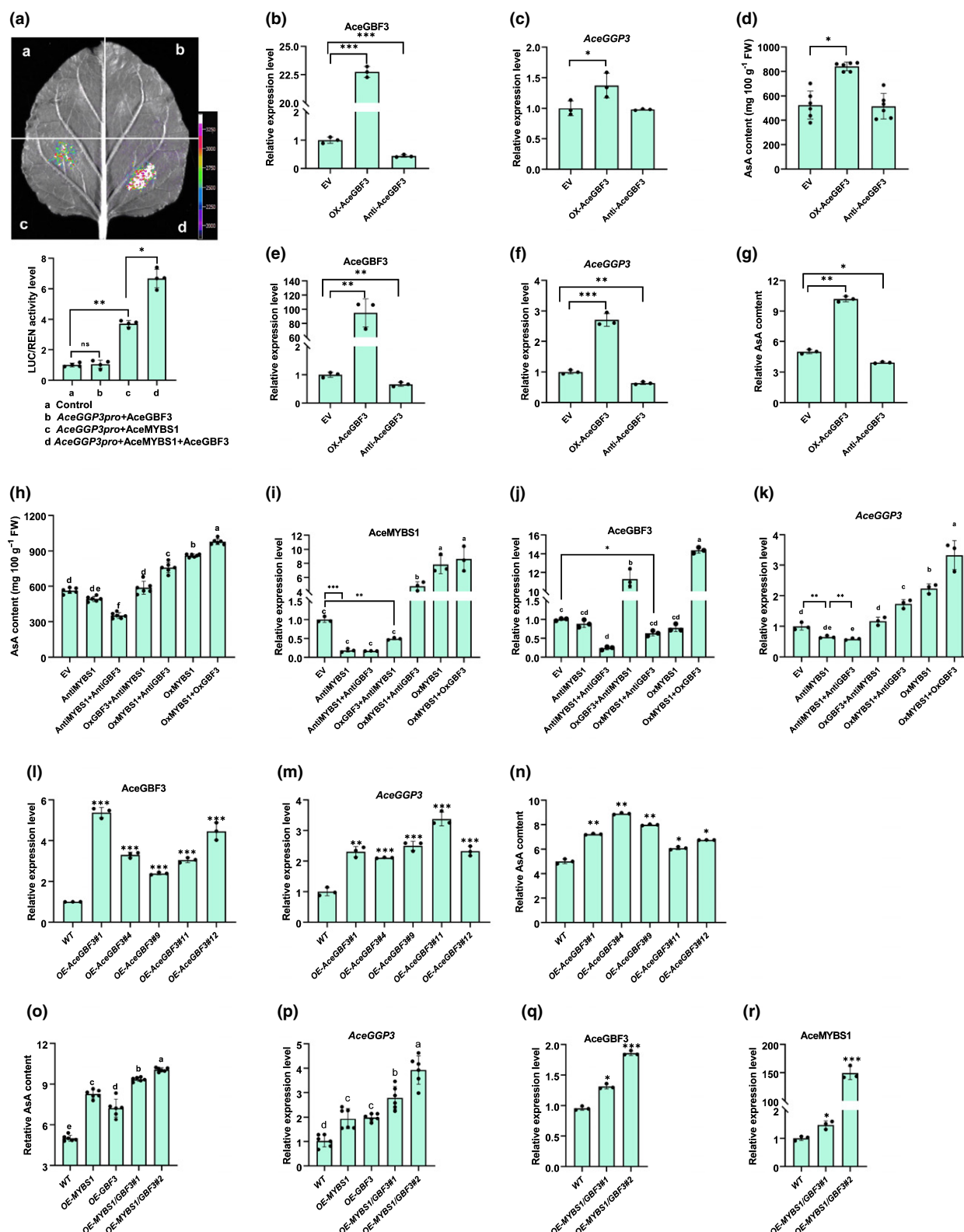


Fig. 6 AceGBF3 interacts with AceMYBS1 to modulate ascorbic acid (AsA) synthesis in an additive manner (GBF, G-box binding factor; MYB, myeloblastosis). (a) Dual-luciferase (LUC) assay in *Nicotiana benthamiana* leaves showing that the transcription of *AceGGP3* is activated by AceMYBS1 and AceGBF3 individually or collectively (representative photographs are above and detected LUC/Renilla Luciferase (REN) activity is below). Quantitative reverse-transcription (qRT)-PCR analysis of (b) *AceGBF3* and (c) *AceGGP3* at 7 d after transformation of *Actinidia eriantha* fruit. EV, empty vector; OX-AceGBF3, AceGBF3-overexpression; Anti-AceGBF3, AceGBF3-antisense expression. (d) AsA content of fruit in (b). Experiments were performed in six kiwifruits per genotype. qRT-PCR analysis of (e) *AceGBF3* and (f) *AceGGP3* in transiently expressed *A. eriantha* calli. (g) Relative AsA content of *A. eriantha* calli in (e). (h) Fruit AsA content of transiently co-expressed AceMYBS1 and AceGBF3 (*A. eriantha*). AceMYBS1-overexpression; AntiMYBS1+AntiGBF3, co-antisense expression AceMYBS1 and AceGBF3; OXMYBS1+OXGBF3, co-overexpression AceMYBS1 and AceGBF3; OXMYBS1+AntiGBF3, AceMYBS1-overexpression in the AceGBF3-antisense expression background; OXGBF3+AntiMYBS1, AceGBF3-overexpression in the AceMYBS1-antisense expression background. Experiments were performed in six kiwifruits per genotype. qRT-PCR analysis of (i) *AceMYBS1*, (j) *AceGBF3* and (k) *AceGGP3* in the fruit in (h). qRT-PCR analysis of (l) *AceGBF3* and (m) *AceGGP3* in transgenic *A. eriantha* calli. WT, wild-type; OE-AceGBF3#1, OE-AceGBF3#4, OE-AceGBF3#9, OE-AceGBF3#11 and OE-AceGBF3#12 represent five independent transgenic lines, respectively. (n) Relative AsA content of AceGBF3-overexpression transgenic calli in (l). (o) Relative AsA content of individual AceMYBS1 and AceGBF3 as well as their co-overexpression in transgenic *A. eriantha* calli. OE-MYBS1/GBF3#1 and OE-MYBS1/GBF3#2, two transgenic lines of AceMYBS1 and AceGBF3 co-overexpression. qRT-PCR analysis expression of (p) *AceGGP3*, (q) *AceGBF3* and (r) *AceMYBS1* in the transgenic kiwifruit calli of OE-AceMYBS1/AceGBF3#2. Error bars represent \pm SD with three technical repeats for each experimental group. Significant differences were detected by Student's *t*-test: *, $P < 0.05$; **, $P < 0.01$; ***, $P < 0.001$; ns, not significant. Different letters above the bars indicate significant difference ($P < 0.05$) as obtain by one-way ANOVA test. Black circles in bar charts represent individual data points.

signalling during seed germination and early seedling development (Yang *et al.*, 2018). MYBS1 is inducible by NaCl, polyethylene glycol or ABA, and regulates the transcription of *AtP5CS* to enhance the salt tolerance of *Arabidopsis* (Dong *et al.*, 2017). These findings suggest that a variety of MYBS1 sequences in different plant species from the same clade are involved in various metabolic mechanisms, and thus a new function in regulating AsA biosynthesis is presented in this study. Overexpression of AceMYBS1 significantly enhanced the expression of *AceGGP3* and the content of AsA (Fig. 4c,d,f,g,j,k) and these levels were reduced when AceMYBS1 was mutated via CRISPR/Cas9 (Fig. 4p). Yeast one-hybrid (Y1H), Dual-luciferase (LUC) and electrophoretic mobility shift assays (EMSA) showed that AceMYBS1 acts by binding the promoter of *AceGGP3* and activates *AceGGP3* transcription (Figs 3, S7).

There is very similar MYBS1 on chr26 which lies within the recently identified high AsA quantitative trait loci (QTL) interval (McCallum *et al.*, 2019) but it has much lower expression than the chr16 AeMYBS1 gene described here. The high similarity suggests that it might also activate *GPP* transcription and the *A. eriantha* allele has some interesting polymorphisms which could alter its TF properties (data not presented here). This locus deserves additional investigation.

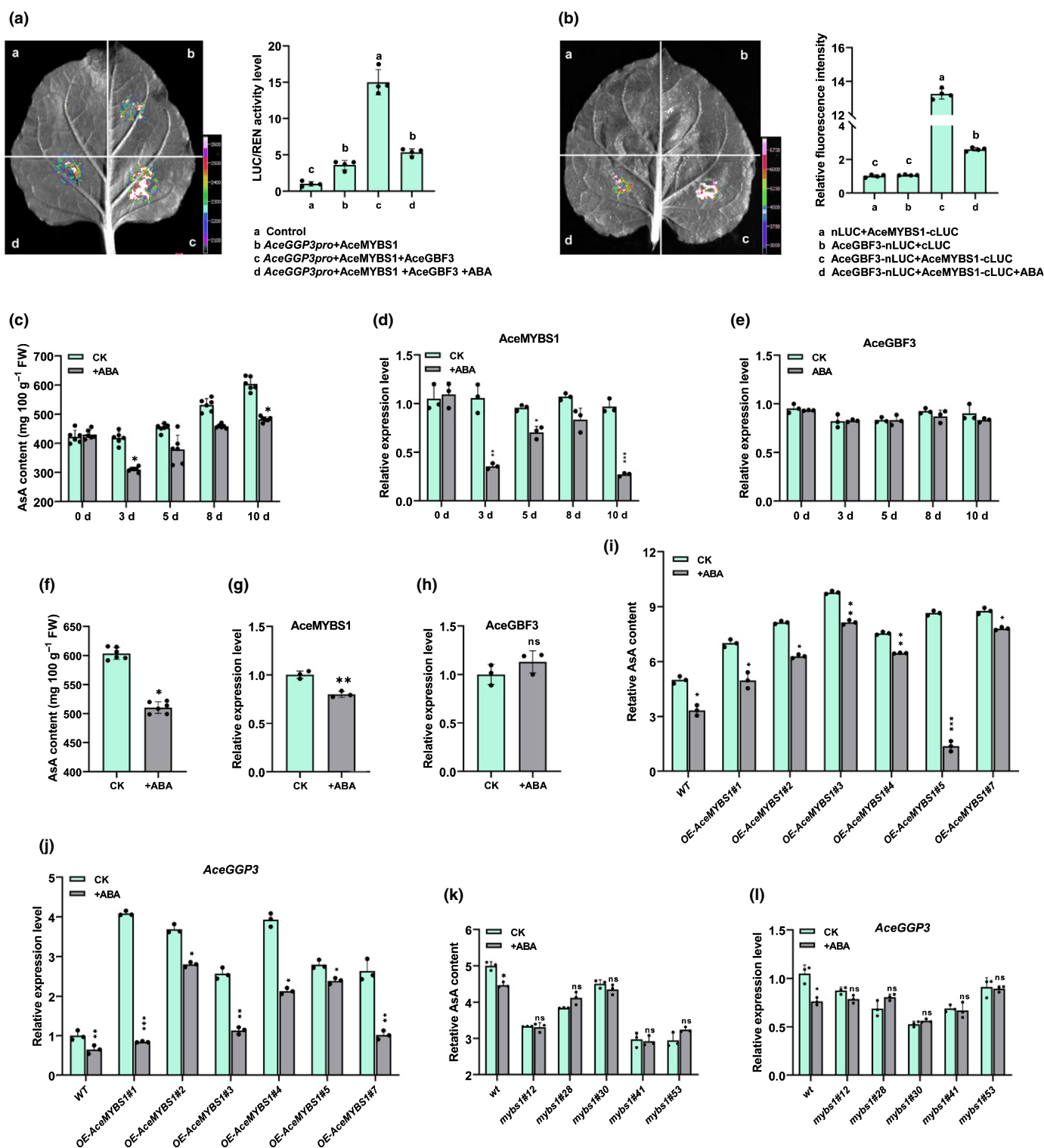
The interaction of AceMYBS1 and AceGBF3 increases the synthesis of AsA in *A. eriantha* in an *AceGGP3*-dependent manner

This study also identified an AceMYBS1-interacting protein, AceGBF3, a member of the bZIP TFs, which also is correlated with the AsA content of *A. eriantha* in different developmental stages (Table S3). G-box binding factor (GBFs) belong to the G-group of bZIP superfamily TFs and have been shown to bind specifically to the G-box sequences in the promoter regions of several environmentally regulated genes in *Arabidopsis* (Menkens *et al.*, 1995; Shinozaki & Yamaguchi-Shinozaki, 1997). To date, GBF3 has been shown, mainly by expression analysis, to participate in light, cold, salt, osmotic and drought stress responses (Lu

et al., 1996; Ma & Bohnert, 2008; Ramegowda *et al.*, 2017). In our study, we found that AceGBF3 interacts together with AceMYBS1 to additively promote AsA synthesis and *AceGGP3* expression (Figs 6h,k,o, S13). Various light, stress and hormone conditions also have been shown to affect the expression of the *GPP*, *GME* and *GPP* genes in kiwifruit (Li *et al.*, 2013a,b), but these studies did not determine the underlying regulatory mechanism(s). Here, we add new knowledge about upstream regulatory factors of *GPPs*, which have developmental-based expression but also respond to exogenous signals to stimulate AsA accumulation in kiwifruit.

ABA represses AsA synthesis by repressing AeMYBS1 expression

ABA is a classic plant hormone that affects the expression of thousands of genes, is widely involved in the process of plant growth, and plays an important role in the abiotic stress response (Dong *et al.*, 2015; Vishwakarma *et al.*, 2017). ABA also affects the synthesis of AsA: a PTP-like nucleotidase (PTPN) mediates the tandem regulation of the ABA signalling pathway and AsA biosynthesis pathway in maize to mediate drought resistance (Zhang *et al.*, 2020). Overexpression of ABA INSENSITIVE 4 (ABI4) was shown to decrease AsA content under salt stress, whereas ETHYLENE INSENSITIVE 3 (EIN3) antagonizes the inhibitory effect of ABA on AsA synthesis (Y. Yu *et al.*, 2019; Kakan *et al.*, 2021). Treatment with ABA and methyl jasmonate (MeJA) significantly reduced AsA content in kiwifruit (Li *et al.*, 2013a) and there also is a feedback response to exogenously elevated AsA in terms of elevated 9-*cis*-Epoxyxycarotenoid Dioxygenase 3 expression (*NCED3*), which results in increased ABA production (Bulley *et al.*, 2021). However, there are few reports on regulators involved in ABA-mediation of AsA synthesis, and the underlying molecular mechanism through which ABA modulates AsA content is unclear. One of the next areas to explore is whether this action by ABA is very direct and limited to AeMYBS1, or whether the regulatory effect is transmitted through a cascade of genes, of which AeMYBS1 is a downstream



member. Gaining a better understanding of such cross-talk will help to better understand the implications for plant biology. This study found that one of the ways in which ABA represses AsA content in fruit tissue is through repressing *AceMYBS1* expression (Figs 7, S15) and how ABA inhibits the expression of *AceMYBS1* is an area for future exploration. This complements studies by other groups which have shown that in roots, at least, ABA

inhibits ascorbate biosynthesis through ABI4-mediated repression of *GGP* expression.

In conclusion, *AceMYBS1* and *AceGBF3* are positive regulators of AsA content, and *AceMYBS1* directly binds the *AceGGP3* promoter and activates its expression, whereas *AceGBF3* interacts together with *AceMYBS1* to additively increase the expression of *AceGGP3* and the synthesis of AsA (Fig. 8). It is well-

Fig. 7 Abscisic acid (ABA) represses ascorbic acid (AsA) biosynthesis by repressing *AeMYBS1* (MYB, myeloblastosis). (a) Dual-luciferase (LUC) assay in *Nicotiana benthamiana* leaves showing the effects on transcription of *AceGGP3* by *AceMYBS1*, *AceMYBS1* and *AceGBF3*, and *AceMYBS1* and *AceGBF3* with 2 μ M ABA (with empty vector as a control) (GBF, G-box binding factor; GGP, GDP-L-galactose-phosphorylase). Left, representative photographs; right, detected LUC/Renilla Luciferase (REN) activity. (b) Bimolecular luminescence complementation (BiLC) assay using *AeGBF3*-nLUC and *AeMYBS1*-cLUC constructs; *Agrobacterium* cultures were combined at a 1 : 1 (v/v) \pm 2 μ M ABA, then infiltrated into *N. benthamiana* leaves. Representative picture shown on left and measured relative fluorescence intensity measured is on right. (c) AsA content of 20 μ M ABA-treated *Actinidia eriantha* fruits over time (CK, sample without ABA treatment). Experiments contained three to six kiwifruits per group. Quantitative reverse-transcription (qRT)-PCR analysis expression of (d) *AceMYBS1* and (e) *AceGBF3* in experimental group in (c). (f) AsA content of *A. eriantha* fruits sprayed with 20 μ M ABA at 80 d after flowering (80 DAF) and stored at 25°C for 3 d. qRT-PCR analysis of (g) *AceMYBS1* and (h) *AceGBF3* expression of fruit in (f). (i) Relative AsA content of *AceMYBS1*-overexpression lines treated with 2 μ M ABA (without ABA is control) (WT, wild-type). (j) qRT-PCR analysis *AceGGP3* in overexpression lines in (i). (k) Relative AsA content of *AceMYBS1* mutant lines treated with 2 μ M ABA (no ABA as a control) (wt, wild-type). (l) qRT-PCR analysis of *AceGGP3* in *AceMYBS1*-edited kiwifruit calli in (k). All of the above experiments were performed in three replicates. Error bars denoted standard deviation (\pm SD). Significant differences were detected by Student's *t*-test: *, $P < 0.05$; **, $P < 0.01$; ***, $P < 0.001$; ns, not significant. Different letters above the bars indicate significant difference ($P < 0.05$) as obtain by one-way ANOVA test. Black circles in bar charts represent individual data points.

documented that developed world diets often are lacking in vitamin C and that improving vitamin C contents in natural dietary sources such as fruit and vegetables is one way to address this. Kiwifruit are very well-known as a rich dietary source and studies using germplasm like this indicate the potential to improve vitamin C contents even more in commercial cultivars.

The other benefit of increasing ascorbate is to increase overall plant resiliency to abiotic stresses such as drought, heat, soil water logging and soil salinity. These stresses are being exacerbated by climate change. Therefore, *AeMYBS1* and *GBF3* transcription factors could be potentially useful new tools for biotech manipulation targeting increased plant resiliency to abiotic stresses.

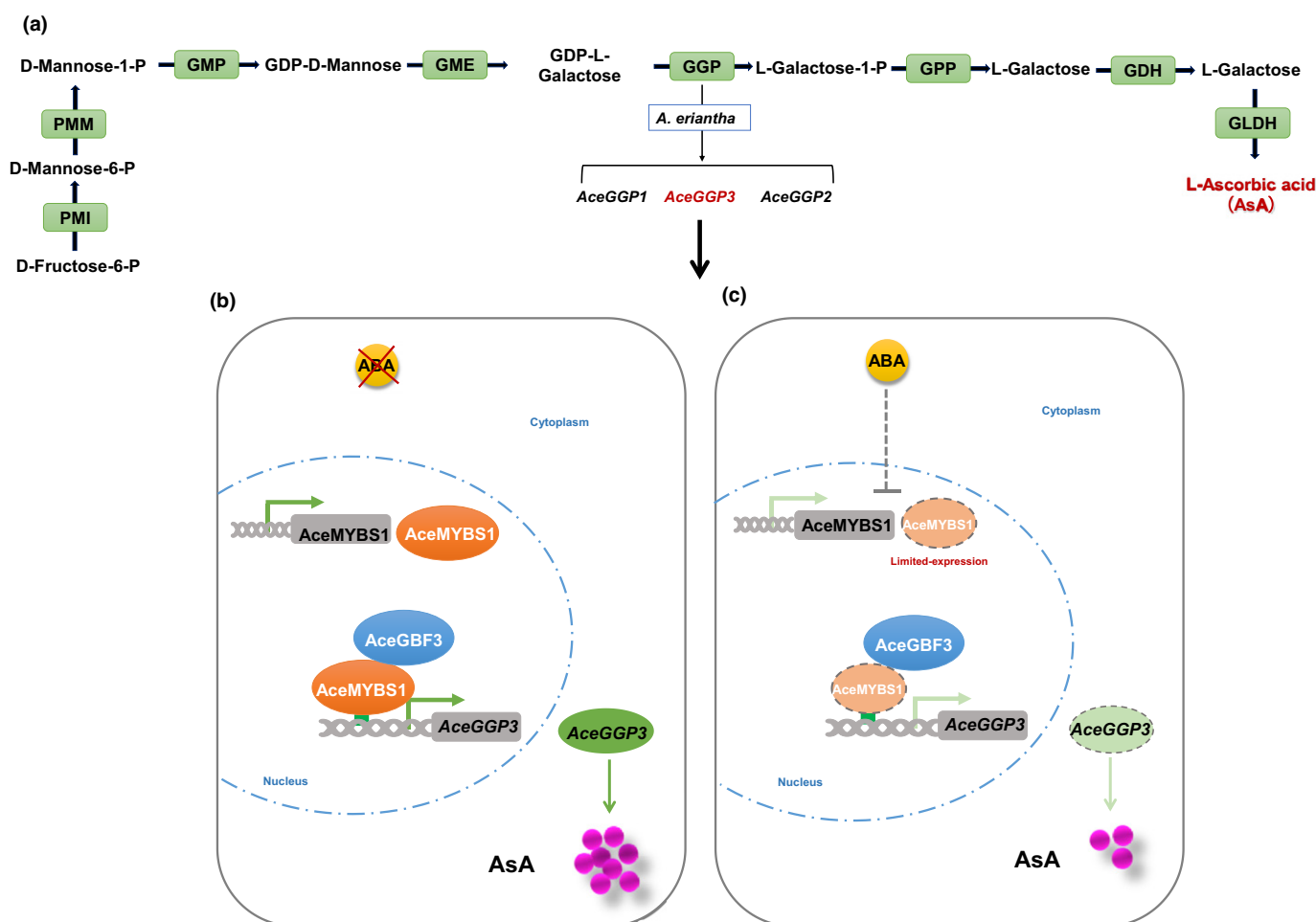


Fig. 8 A working model of abscisic acid (ABA)-mediated *AceGBF3*-*AceMYBS1*-*AceGGP3* networks regulating the AsA synthesis in kiwifruit (*Actinidia eriantha*) (GBF, G-box binding factor; GGP, GDP-L-galactose-phosphorylase; MYB, myeloblastosis). (a) AsA biosynthetic genes of the L-galactose pathway. (b) *AceMYBS1* binds to the *AceGGP3* promoter (position signified by green arrow) and activates the expression of *AceGGP3*, thereby promoting AsA synthesis. *AceGBF3* interacts with *AceMYBS1* to further activate the *AceGGP3* expression and enhance AsA synthesis. Without exogenous ABA, the *AceGBF3*-*AceMYBS1*-*AceGGP3* networks positively regulate AsA synthesis. (c) In the presence of ABA, *AceMYBS1* is repressed, resulting in reduced AsA synthesis.


Acknowledgements

The authors would like to thank the referees for their comments and suggestions. The authors also thank William Laing for comments and suggestions to manuscript as well as the PFR Science Publication Office staff for proof reading and formatting. This project was supported by the National Key R&D Program of China (2019YFD1000201) and Science and Technology Department of Hubei Province (2020DFE016).

Author contributions

DL and XL planned and designed the research; XL, CZ and DL performed experiments and conducted fieldwork; XL, SMB, RW and DL analyzed data; and DL and SMB wrote the manuscript.

ORCID

Sean M. Bulley  <https://orcid.org/0000-0001-6142-5414>

Dawei Li  <https://orcid.org/0000-0002-5138-4492>

Data availability

The data that support the findings of this study are available in the supplementary material of this article. RNAseq data are openly available in NCBI at <https://www.ncbi.nlm.nih.gov>, GenBank accession no. PRJNA771781 and PRJNA771785.

References

- Aguius F, Gonzalez-Lamothe R, Caballero J, Munoz-Blanco J, Botella M, Valpuesta V. 2003. Engineering increased vitamin C levels in plants by overexpression of a D-galacturonic acid reductase. *Nature Biotechnology* 21: 177–181.
- Akbaş F, Isikalan C, Namli S. 2009. Callus induction and plant regeneration from different explants of *Actinidia deliciosa*. *Applied Biochemistry and Biotechnology* 158: 470–475.
- An JP, Zhang XW, You CX, Bi SQ, Wang XF, Hao YJ. 2019. MdWRKY40 promotes wounding-induced anthocyanin biosynthesis in association with MdMYB1 and undergoes MdbT2-mediated degradation. *New Phytologist* 224: 380–395.
- Badejo AA, Jeong ST, Goto-Yamamoto N, Esaka M. 2007. Cloning and expression of GDP-d-mannose pyrophosphorylase gene and ascorbic acid content of acerola (*Malpighia glabra* L.) fruit at ripening stages. *Plant Physiology and Biochemistry* 45: 665–672.
- Barth C, De Tullio M, Conklin PL. 2006. The role of ascorbic acid in the control of flowering time and the onset of senescence. *Journal of Experimental Botany* 57: 1657–1665.
- Boyer LA, Langer MR, Crowley KA, Tan S, Denu JM, Peterson CL. 2002. Essential role for the SANT domain in the functioning of multiple chromatin remodeling enzymes. *Molecular Cell* 10: 935–942.
- Boyer LA, Latek RR, Peterson CL. 2004. The SANT domain: a unique histone-tail-binding module? *Nature Reviews Molecular Cell Biology* 5: 158–163.
- Bu Y, Sun B, Zhou A, Zhang X, Takano T, Liu S. 2016. Overexpression of *AtOxR* gene improves abiotic stresses tolerance and vitamin C content in *Arabidopsis thaliana*. *BMC Biotechnology* 16: 69.
- Bulley SM, Cooney JM, Laing W. 2021. Elevating ascorbate in *Arabidopsis* stimulates the production of abscisic acid, phaseic acid, and to a lesser extent auxin (IAA) and jasmonates, resulting in increased expression of DHAR1 and multiple transcription factors associated with abiotic stress tolerance. *International Journal of Molecular Sciences* 22: 6743.
- Bulley S, Laing W. 2016. The regulation of ascorbate biosynthesis. *Current Opinion in Plant Biology* 33: 15–22.
- Bulley SM, Rassam M, Hoser D, Otto W, Schunemann N, Wright M, MacRae E, Gleave A, Laing W. 2009. Gene expression studies in kiwifruit and gene over-expression in *Arabidopsis* indicates that GDP-L-galactose guanylttransferase is a major control point of vitamin C biosynthesis. *Journal of Experimental Botany* 60: 765–778.
- Bulley S, Wright M, Rommens C, Yan H, Rassam M, Lin-Wang K, Andre C, Brewster DI, Karunaitnam S, Allan AC *et al.* 2012. Enhancing ascorbate in fruits and tubers through over-expression of the L-galactose pathway gene *GDP-L-galactose phosphorylase*. *Plant Biotechnology Journal* 10: 390–397.
- Cai X, Zhang C, Ye J, Hu T, Ye Z, Li H, Zhang Y. 2015. Ectopic expression of *FaGalUR* leads to ascorbate accumulation with enhanced oxidative stress, cold, and salt tolerance in tomato. *Plant Growth Regulation* 76: 187–197.
- Carr AC, Maggini S. 2017. Vitamin C and immune function. *Nutrients* 9: 1211.
- Castro JC, Cobos M, Maddox JD, Imán SA, Egoavil A, Torres J, Gutierrez F. 2015. Gene expression and enzyme activities of the D-mannose/L-galactose pathway influence L-ascorbic acid content in *Myrciaria dubia*. *Biologia Plantarum* 59: 783–787.
- Chen H, Zou Y, Shang Y, Lin H, Wang Y, Cai R, Tang X, Zhou JM. 2008. Firefly luciferase complementation imaging assay for protein-protein interactions in plants. *Plant Physiology* 146: 368–376.
- Chen W, Hu T, Ye J, Wang B, Liu G, Wang Y, Yuan L, Li J, Li F, Ye Z *et al.* 2020. A CCAAT-binding factor, SINFYA10, negatively regulates ascorbate accumulation by modulating the D-mannose/L-galactose pathway in tomato. *Horticulture Research* 7: 200.
- Chen Y, Shu P, Wang R, Du X, Xie Y, Du K, Deng H, Li M, Zhang Y, Grierson D *et al.* 2021. Ethylene response factor AcERF91 affects ascorbate metabolism via regulation of GDP-galactose phosphorylase encoding gene (*AcGGP3*) in kiwifruit. *Plant Science* 313: 111063.
- Cheng C, Yu Q, Wang Y, Wang H, Dong Y, Ji Y, Zhou X, Li Y, Jiang CZ, Gan SS *et al.* 2021. Ethylene-regulated asymmetric growth of the petal base promotes flower opening in rose (*Rosa hybrida*). *Plant Cell* 33: 1229–1251.
- De Tullio MC. 2012. Beyond the antioxidant: the double life of vitamin C. *Subcellular Biochemistry* 56: 49–65.
- Dong T, Park Y, Hwang I. 2015. Abscicic acid: biosynthesis, inactivation, homeostasis and signalling. *Essays in Biochemistry* 58: 29–48.
- Dong W, Song Y, Zhao Z, Qiu NW, Liu X, Guo W. 2017. The *Medicago truncatula* R2R3-MYB transcription factor gene *MtMYBS1* enhances salinity tolerance when constitutively expressed in *Arabidopsis thaliana*. *Biochemical and Biophysical Research Communications* 490: 225–230.
- Dowdle J, Ishikawa T, Gatzek S, Rolinski S, Smirnoff N. 2007. Two genes in *Arabidopsis thaliana* encoding GDP-L-galactose phosphorylase are required for ascorbate biosynthesis and seedling viability. *The Plant Journal* 52: 673–689.
- Du G, Li M, Ma F, Liang D. 2009. Antioxidant capacity and the relationship with polyphenol and Vitamin C in *Actinidia* fruits. *Food Chemistry* 113: 557–562.
- Fenech M, Amorim-Silva V, Esteban del Valle A, Arnaud D, Ruiz-Lopez N, Castillo AG, Smirnoff N, Botella MA. 2021. The role of GDP-L-galactose phosphorylase in the control of ascorbate biosynthesis. *Plant Physiology* 185: 1574–1594.
- Fornes O, Castro-Mondragon JA, Khan A, van der Lee R, Zhang XI, Richmond PA, Modi BP, Correard S, Gheorghe M, Baranašić D *et al.* 2019. JASPAR 2020: update of the open-access database of transcription factor binding profiles. *Nucleic Acids Research* 48: D87–D92.
- Fu X, Peng B, Hassani D, Xie L, Liu H, Li Y, Chen T, Liu P, Tang Y, Li L *et al.* 2021. AaWRKY9 contributes to light- and jasmonate-mediated to regulate the biosynthesis of artemisinin in *Artemisia annua*. *New Phytologist* 231: 1858–1874.
- Gao Y, Wei W, Fan Z, Zhao X, Zhang Y, Jing Y, Zhu B, Zhu H, Shan W, Chen J *et al.* 2020. Re-evaluation of the nor mutation and the role of the NAC-NOR transcription factor in tomato fruit ripening. *Journal of Experimental Botany* 71: 3560–3574.
- Geng J, Liu JH. 2018. The transcription factor CsbHLH18 of sweet orange functions in modulation of cold tolerance and homeostasis of reactive oxygen

- species by regulating the antioxidant gene. *Journal of Experimental Botany* 69: 2677–2692.
- Gietz RD, Schiestl RH. 2007. High-efficiency yeast transformation using the LiAc/SS carrier DNA/PEG method. *Nature Protocols* 2: 31–34.
- Gill SS, Tuteja N. 2010. Reactive oxygen species and antioxidant machinery in abiotic stress tolerance in crop plants. *Plant Physiology and Biochemistry* 48: 909–930.
- Green MA, Fry SC. 2005a. Apoplastic degradation of ascorbate: novel enzymes and metabolites permeating the plant cell wall. *Plant Biosystems* 139: 2–7.
- Green MA, Fry SC. 2005b. Vitamin C degradation in plant cells via enzymatic hydrolysis of 4-O-oxalyl-L-threonate. *Nature* 433: 83–87.
- Hellens RP, Allan AC, Friel EN, Bolitho K, Grafton K, Templeton MD, Karunairatnam S, Gleave AP, Laing WA. 2005. Transient expression vectors for functional genomics, quantification of promoter activity and RNA silencing in plants. *Plant Methods* 1: 1–14.
- Hong Y-F, Ho T-HD, Wu C-F, Ho S-L, Yeh R-H, Lu C-A, Chen P-W, Yu L-C, Chao A, Yu S-M. 2012. Convergent starvation signals and hormone crosstalk in regulating nutrient mobilization upon germination in cereals. *Plant Cell* 24: 2857–2873.
- Horemans N, Foyer CH, Potters G, Asard H. 2000. Ascorbate function and associated transport systems in plants. *Plant Physiology and Biochemistry* 38: 531–540.
- Hu T, Ye J, Tao P, Li H, Zhang J, Zhang Y, Ye Z. 2016. The tomato HD-Zip I transcription factor SHZ24 modulates ascorbate accumulation through positive regulation of the D-mannose/L-galactose pathway. *The Plant Journal* 85: 16–29.
- Huang H, Wang Y, Zhang Z, Jiang Z, Wang S. 2004. *Actinidia germplasm resources and kiwifruit industry in China*. *HortScience* 39: 1165–1172.
- Kakan X, Yu Y, Li S, Li X, Huang R, Wang J. 2021. Ascorbic acid modulation by ABI4 transcriptional repression of VTC2 in the salt tolerance of Arabidopsis. *BMC Plant Biology* 21: 1–12.
- Ko ER, Ko D, Chen C, Lipsick JS. 2008. A conserved acidic patch in the Myb domain is required for activation of an endogenous target gene and for chromatin binding. *Molecular Cancer* 7: 1–20.
- Kotchoni SO, Larrimore KE, Mukherjee M, Kempinski CF, Barth C. 2009. Alterations in the endogenous ascorbic acid content affect flowering time in Arabidopsis. *Plant Physiology* 149: 803–815.
- Kumar S, Stecher G, Tamura K. 2016. MEGA7: molecular evolutionary genetics analysis v.7.0 for bigger datasets. *Molecular Biology and Evolution* 33: 1870–1874.
- Laing WA, Martínez-Sánchez M, Wright MA, Bulley SM, Brewster DI, Dare AP, Rassam M, Wang D, Storey R, Macknight RC *et al.* 2015. An upstream open reading frame is essential for feedback regulation of ascorbate biosynthesis in Arabidopsis. *Plant Cell* 27: 772–786.
- Laing WA, Wright MA, Cooney J, Bulley SM. 2007. The missing step of the L-galactose pathway of ascorbate biosynthesis in plants, an L-galactose guanylyltransferase, increases leaf ascorbate content. *Proceedings of the National Academy of Sciences, USA* 104: 9534–9539.
- Latocha P, Krupa T, Wołosiak R, Worobiej E, Wilczak J. 2010. Antioxidant activity and chemical difference in fruit of different *Actinidia* sp. *International Journal of Food Sciences and Nutrition* 61: 381–394.
- Letunic I, Khedkar S, Bork P. 2020. SMART: recent updates, new developments and status in 2020. *Nucleic Acids Research* 49: D458–D460.
- Li J, Cui M, Li M, Wang X, Liang D, Ma F. 2013a. Expression pattern and promoter analysis of the gene encoding GDP-D-mannose 3',5'-epimerase under abiotic stresses and applications of hormones by kiwifruit. *Scientia Horticulturae* 150: 187–194.
- Li J, Liang D, Li M, Ma F. 2013b. Light and abiotic stresses regulate the expression of GDP-L-galactose phosphorylase and levels of ascorbic acid in two kiwifruit genotypes via light-responsive and stress-inducible cis-elements in their promoters. *Planta* 238: 535–547.
- Li S, Wang J, Yu Y, Wang F, Dong J, Huang R. 2016. D27E mutation of VTC1 impairs the interaction with CSN5B and enhances ascorbic acid biosynthesis and seedling growth in Arabidopsis. *Plant Molecular Biology* 92: 473–482.
- Lin R, Ding L, Casola C, Ripoll DR, Feschotte C, Wang H. 2007. Transposase-derived transcription factors regulate light signaling in Arabidopsis. *Science* 318: 1302–1305.
- Linster CL, Gomez TA, Christensen KC, Adler LN, Young BD, Brenner C, Clarke SG. 2007. Arabidopsis VTC2 encodes a GDP-L-galactose phosphorylase, the last unknown enzyme in the Smirnoff-wheeler pathway to ascorbic acid in plants. *Journal of Biological Chemistry* 282: 18879–18885.
- Liu X, Xie X, Zhong C, Li D. 2021. Comparative transcriptome analysis revealed the key genes regulating ascorbic acid synthesis in *Actinidia*. *International Journal of Molecular Sciences* 22: 12894.
- Lorence A, Chevone B, Mendes P, Nessler C. 2004. Myo-inositol oxygenase offers a possible entry point into plant ascorbate biosynthesis. *Plant Physiology* 134: 1200–1205.
- Lu C-A, T-HD HO, Ho S-L, Yu S-M. 2002. Three novel MYB proteins with one DNA binding repeat mediate sugar and hormone regulation of alpha-amylase gene expression. *Plant Cell* 14: 1963–1980.
- Lu G, Paul AL, McCarty DR, Ferl RJ. 1996. Transcription factor veracity: is GBF3 responsible for ABA-regulated expression of Arabidopsis Adh? *Plant Cell* 8: 847–857.
- Ma S, Bohnert HJ. 2008. Gene networks in *Arabidopsis thaliana* for metabolic and environmental functions. *Molecular Biosystems* 4: 199–204.
- Macknight RC, Laing WA, Bulley SM, Broad RC, Johnson AAT, Hellens RP. 2017. Increasing ascorbate levels in crops to enhance human nutrition and plant abiotic stress tolerance. *Current Opinion in Biotechnology* 44: 153–160.
- McCallum J, Laing W, Bulley S, Thomson S, Catanach A, Shaw M, Knaebel M, Tahir J, Deroles S, Timmerman-Vaughan G *et al.* 2019. Molecular characterisation of a supergene conditioning super-high vitamin C in kiwifruit hybrids. *Plants* 8: 237.
- Mellidou I, Kanellis AK. 2017. Genetic control of ascorbic acid biosynthesis and recycling in horticultural crops. *Frontiers in Chemistry* 5: 50.
- Menkens AE, Schindler U, Cashmore AR. 1995. The G-box: a ubiquitous regulatory DNA element in plants bound by the GBF family of bZIP proteins. *Trends in Biochemical Sciences* 20: 506–510.
- Mitsuda N, Ohme-Takagi M. 2009. Functional analysis of transcription factors in Arabidopsis. *Plant and Cell Physiology* 50: 1232–1248.
- Mittler R. 2002. Oxidative stress, antioxidants and stress tolerance. *Trends in Plant Science* 7: 405–410.
- Moser MA, Chun OK. 2016. Vitamin C and heart health: a review based on findings from epidemiologic studies. *International Journal of Molecular Sciences* 17: 1328.
- Myint PK, Luben RN, Welch AA, Bingham SA, Wareham NJ, Khaw K-T. 2008. Plasma vitamin C concentrations predict risk of incident stroke over 10 y in 20 649 participants of the European prospective investigation into cancer Norfolk prospective population study. *American Journal of Clinical Nutrition* 87: 64–69.
- Pilkington SM, Crowhurst R, Hilario E, Nardoza S, Fraser L, Peng Y, Gunaseelan K, Simpson R, Tahir J, Deroles SC *et al.* 2018. A manually annotated *Actinidia chinensis* var. *chinensis* (kiwifruit) genome highlights the challenges associated with draft genomes and gene prediction in plants. *BMC Genomics* 19: 1–19.
- Pullar JM, Carr AC, Vissers MCM. 2017. The roles of vitamin C in skin health. *Nutrients* 9: 866.
- Queval G, Noctor G. 2007. A plate reader method for the measurement of NAD, NADP, glutathione, and ascorbate in tissue extracts: application to redox profiling during Arabidopsis rosette development. *Analytical Biochemistry* 363: 58–69.
- Ramegowda V, Gill US, Sivalingam PN, Gupta A, Gupta C, Govind G, Nataraja KN, Pereira A, Udayakumar M, Mysore KS *et al.* 2017. GBF3 transcription factor imparts drought tolerance in *Arabidopsis thaliana*. *Scientific Reports* 7: 9148.
- Sanmartin M, Drogoudi PA, Lyons T, Pateraki I, Barnes J, Kanellis AK. 2003. Over-expression of ascorbate oxidase in the apoplast of transgenic tobacco results in altered ascorbate and glutathione redox states and increased sensitivity to ozone. *Planta* 216: 918–928.
- Schultz J, Milpetz F, Bork P, Ponting CP. 1998. SMART, a simple modular architecture research tool: identification of signaling domains. *Proceedings of the National Academy of Sciences, USA* 95: 5857–5864.
- Shinozaki K, Yamaguchi-Shinozaki K. 1997. Gene expression and signal transduction in water-stress response. *Plant Physiology* 115: 327–334.
- Smirnoff. 2011. Vitamin C: the metabolism and functions of ascorbic acid in plants. *Advances in Botanical Research* 59: 107–177.

- Troesch B, Hoefft B, McBurney M, Eggersdorfer M, Weber P. 2012. Dietary surveys indicate vitamin intakes below recommendations are common in representative Western countries. *British Journal of Nutrition* 108: 692–698.
- Venkatesh J, Park SW. 2014. Role of L-ascorbate in alleviating abiotic stresses in crop plants. *Botanical Studies* 55: 38.
- Vishwakarma K, Upadhyay N, Kumar N, Yadav G, Singh J, Mishra RK, Kumar V, Verma R, Upadhyay RG, Pandey M *et al.* 2017. Abscisic acid signaling and abiotic stress tolerance in plants: a review on current knowledge and future prospects. *Frontiers in Plant Science* 8: 161.
- Wang X, Tu M, Wang D, Liu J, Li Y, Li Z, Wang Y, Wang X. 2018. CRISPR/Cas9-mediated efficient targeted mutagenesis in grape in the first generation. *Plant Biotechnology Journal* 16: 844–855.
- Wang Z, Wang S, Li D, Zhang Q, Li L, Zhong C, Liu Y, Huang H. 2018. Optimized paired-sgRNA/Cas9 cloning and expression cassette triggers high-efficiency multiplex genome editing in kiwifruit. *Plant Biotechnology Journal* 16: 1424–1433.
- Wheeler GL, Jones MA, Smirnoff N. 1998. The biosynthetic pathway of vitamin C in higher plants. *Nature* 393: 365–369.
- Xu C. 2020. Pull-down and co-immunoprecipitation assays of interacting proteins in plants. *Chinese Bulletin of Botany* 55: 62–68.
- Yang B, Song Z, Li C, Jiang J, Zhou Y, Wang R, Wang Q, Ni C, Liang Q, Chen H *et al.* 2018. RSM1, an Arabidopsis MYB protein, interacts with HY5/HYH to modulate seed germination and seedling development in response to abscisic acid and salinity. *PLoS Genetics* 14: e1007839.
- Ye J, Li W, Ai G, Li C, Liu G, Chen W, Wang B, Wang W, Lu Y, Zhang J *et al.* 2019. Genome-wide association analysis identifies a natural variation in basic helix-loop-helix transcription factor regulating ascorbate biosynthesis via D-mannose/L-galactose pathway in tomato. *PLoS Genetics* 15: e1008149.
- Yu M, Man Y, Wang Y. 2019. Light- and temperature-induced expression of an R2R3-MYB gene regulates anthocyanin biosynthesis in red-fleshed kiwifruit. *International Journal of Molecular Sciences* 20: 5228.
- Yu Y, Wang J, Li S, Kakan X, Zhou Y, Miao Y, Wang F, Qin H, Huang R. 2019. Ascorbic acid integrates the antagonistic modulation of ethylene and abscisic acid in the accumulation of reactive oxygen species. *Plant Physiology* 179: 1861–1875.
- Yuan J, Yu Z, Lin T, Wang L, Chen X, Liu T, Wang J, Hou X, Li Y. 2020. BcERF070, a novel ERF (ethylene-response factor) transcription factor from non-heading Chinese cabbage, affects the accumulation of ascorbic acid by regulating ascorbic acid-related genes. *Molecular Breeding* 40: 1–18.
- Zhang G-Y, Liu R-R, Zhang C-Q, Tang K-X, Sun M-F, Yan G-H, Liu Q-Q. 2015. Manipulation of the rice L-galactose pathway: evaluation of the effects of transgene overexpression on ascorbate accumulation and abiotic stress tolerance. *PLoS ONE* 10: e0125870.
- Zhang H, Xiang Y, He N, Liu X, Liu H, Fang L, Zhang F, Sun X, Zhang D, Li X *et al.* 2020. Enhanced vitamin C production mediated by an ABA-induced PTP-like nucleotidase improves plant drought tolerance in Arabidopsis and maize. *Molecular Plant* 13: 760–776.
- Zhang W, Lorence A, Gruszewski HA, Chevone BI, Nessler CL. 2009. *AMR1*, an Arabidopsis gene that coordinately and negatively regulates the mannose/L-galactose ascorbic acid biosynthetic pathway. *Plant Physiology* 150: 942–950.
- Zhang Z, Wang J, Zhang R, Huang R. 2012. The ethylene response factor AtERF98 enhances tolerance to salt through the transcriptional activation of ascorbic acid synthesis in Arabidopsis. *The Plant Journal* 71: 273–287.
- Zhou Y, Tao QC, Wang ZN, Fan R, Li Y, Sun XF, Tang KX. 2012. Engineering ascorbic acid biosynthetic pathway in Arabidopsis leaves by single and double gene transformation. *Biologia Plantarum* 56: 451–457.
- Zhu W, Zhou H, Lin F, Zhao X, Jiang Y, Xu D, Deng XW. 2020. COLD-REGULATED GENE27 integrates signals from light and the circadian clock to promote hypocotyl growth in Arabidopsis. *Plant Cell* 32: 3155–3169.

Supporting Information

Additional Supporting Information may be found online in the Supporting Information section at the end of the article.

Fig. S1 Differentially expressed genes.

Fig. S2 Expression of *GGP1*, *GGP3* and AsA content.

Fig. S3 Gene expression in *Actinidia eriantha* and *A. rufa* hybrids.

Fig. S4 Transient expression *AceGGP3* in *Actinidia eriantha* calli.

Fig. S5 Correlation and phylogenetic analysis of AceMYBS1.

Fig. S6 Disorder and ‘SMART’ domain architecture predictions.

Fig. S7 AceMYBS1 activated the *AceGGP3* promoter.

Fig. S8 The predicted binding sequence motif of AceMYBS1.

Fig. S9 Phylogenetic analysis of GBF3.

Fig. S10 AceMYBS1 interacts with AceGBF3.

Fig. S11 Subcellular localization of AceMYBS1 and AceGBF3 protein.

Fig. S12 Transiently overexpressed *AceGBF3* in tobacco.

Fig. S13 Transiently overexpressed *AceGBF3*, *AceMYBS1* and co-expression in tobacco leaves.

Fig. S14 ABA inhibits AsA synthesis.

Fig. S15 ABA inhibits AsA synthesis via AceMYBS1.

Methods S1 Details of methods.

Notes S1 Promoter sequence of *AceGGP3*; CDS of *AcrGGP3*; CDS of *AcrGGP1*; CDS of *AcrGGP2* in fasta format.

Table S1 Sequences of primers and other oligonucleotides used in this study.

Table S2 The GenBank accession numbers used in this study.

Table S3 The summary of the expression profile of transcript factors that was related with AsA and the correlation coefficient between these transcript factor and GGP3.

Please note: Wiley Blackwell are not responsible for the content or functionality of any Supporting Information supplied by the authors. Any queries (other than missing material) should be directed to the *New Phytologist* Central Office.